Malaysian Journal of Chemistry, 2020, Vol. 22(2), 121-162

Application of Single–Walled Carbon Nanotubes (SWCNT) in the Production of Glucose Biosensors and Improving Their Performance Using Gold Colloidal Nanoparticles and Usage of Polyaniline Nanostructure–Based Biosensors for Detecting Glucose and Cholesterol

Alireza Heidari[1,2*]
[1]Faculty of Chemistry, California South University, 14731 Comet St., Irvine, CA 92604, USA
[2]American International Standards Institute, Irvine, CA 3800, USA
*Corresponding author (e-mail: scholar.researcher.scientist@gmail.com)

In this study, glucose oxidase was used as stabilization medium due to its higher efficiency, ability for more accurate control of enzyme reaction, protecting against wasting of enzyme as well as simple and easy use and exchange of enzyme medium after performing some levels of surface modification and developing single–walled carbon nanotubes (SWCNT) on gold plates. For better connecting and stabilizing of the enzyme on the medium, the prepared medium was washed with concentrated sulfuric acid and nitric acid and a large volume of deionized water. For protecting the enzyme from devastating effects of gold and prohibiting it from becoming inactive, the surface was covered with cystamine before stabilization. Regarding the large size of glucose oxidase compared to the surface of the medium, a connective material with amid at one end and pyrine at the other end was used as a transfer agent, and for stabilizing this connection the prepared medium was placed into dimethylformamide (DMF) solution for a couple of hours. Activity of the stabilized enzyme at the wavelength of 460 nm recorded by spectroscope was depicted against time to evaluate its stability at various times. The prepared medium, which had a large amount of glucose oxidase, could be used as an electrode in sensors. Furthermore, glucose oxidase electrochemical sensor is one of the best methods for detecting low amounts of glucose, and applying gold colloidal nanoparticles as a supplementary material in the structure of biosensors can be effective for improving its efficiency and optimum performance. In this study, a modified carbon paste electrode biosensor with gold colloidal nanoparticles (A_{unano}/CPE) was produced by carbon graphite powder, paraffin oil and, gold colloidal nanoparticles (24 nm), and was compared with carbon paste electrode (CP). In semi–permeable membranes, a combination of 1 ml of 0.1 M phosphate buffer with specified pH and 10 mg of glucose oxidase was placed around each electrode. At the same potential of 0.7 V, biosensors were tested with glucose in the concentration range of 0–1 mM and various pH (4, 6, and 8), which led to the production of the maximum current and tracing glucose at pH=6 and concentration of 1 M as the optimum condition. Currentmetry induced from both biosensors was compared and confirmed that using gold colloidal nanoparticles in the structure of A_{unano}/CPE electrode led to the increase of the conductivity and currentmerty of the biosensors. Qualitative and quantitative measurement of food components is of great importance due to high cost of traditional methods, in addition to tendency for more accurate and sensitive detecting of these components. Glucose and cholesterol are such compounds that are frequently measured. Various methods are used to detect these food elements, however the necessity for accurate measurement of these two compounds with high sensitivity, especially for food health issues, leads to the development of biological methods, especially biosensors. Among them, biosensors based on conductive polymer nanostructures, especially polyaniline, have been recently gained interest due to their unique characteristics. The current paper aims to introduce and investigate the previously performed studies about polyaniline–based biosensors for detecting glucose and cholesterol.

Key words: Single–Walled Carbon Nanotube (SWCNT); glucose oxidase; Vapor Phase Precipitation; biosensor; gold colloidal nanoparticles; currentmetry; glucose; cholesterol; polyaniline nanofibers; polyaniline nanotubes

Received: May 2020; Accepted: June 2020

In recent decades, biosensors have been manufactured in very small scales (nanometers) as nanotechnology is introduced into biological sciences. Nanobiosensors are very small sensors in nanometer scale that are able to detect special chemicals and/or biological matters with very high accuracy and in completely selective form by stabilizing enzymes, and/or any other cell products on their surfaces [1–11].

Carbon nanotubes are one of the most frequent and appropriate nanostructures which can be used to make nano–biosensors due to their physical and chemical characteristics.

However, appropriate tests must be done to demonstrate their abilities. One of their clear advantages is that they have a large operational area, especially single–walled carbon nanotubes (SWCNT). Stabilizing biological detectors such as enzymes over these materials may lead to the increase in the performance of enzyme reaction, controllability of reaction, participation of more enzymes in reaction, and prohibiting enzymes from wasting as well as information transferring with higher rate in these nano–biosensors [12–17].

Carbon nanotubes should be stabilized on a surface for better action as the base of sensors. Stabilizing surfaces are mainly metallic. In the current paper, gold plate was used for this purpose. Various methods have been used for developing and stabilizing carbon nanotubes on the media. However, the most frequently used method is chemical vapor deposition (CVD) [17–22].

Electrostatic, hydrophobic reactions, and/or covalent bond along with oxidization of nanotubes are mainly used for stabilizing large enzymes on the surface of carbon nanotubes and a simple absorption on the external surface. In these types of bonds, a connective material is mainly used [23–27].

In the structure of nano–biosensors, the covered surfaces of the media by nanotubes are responsible for transferring the effects induced by reaction to transducer devices for illustrating the signal. Carbon nanotubes can play dual roles, as the location of enzyme stabilization and connective limit between reagent and transducer [24, 25].

Biosensor technology is promisingly developed in bio–analytical researches. Sensors or biosensors are used for illustrating various analytes in various times. In 2012, glass carbon (GC) electrode biosensor, multi–walled carbon nanotube (MWCNT), titanium dioxide (TiO_2), apatite hydroxide, and glucose oxidase (GOX) were produced in China based on this technology [28–31]. A chemical sensor consists of receiver, transducer, and separator. Receiver or the biological element such as an enzyme establishes a biological connection with the measureable component. Transducer converts the measurable component into optical or electric signals and separator can acts as a membrane [32–35]. In 2012, an electrode biosensor was produced in South Africa based on glass carbon, multi–walled carbon nanotube (MWCNT), nickel nanoparticle, and glucose oxidase and the amount of glucose in the compound was measured through electric signals using ammeters [36–39]. In 2011, a biosensor was produced in Taiwan based on glass carbon working electrode, glutaraldehyde (GA), carbon nanotube (multi–walled–gelatin), and glucose oxidase (GOX) [40]. Glucose biosensor is one of the most successful biosensors in detecting chemical compounds such as glucose at very low amounts. Its efficiency and sensitivity can be considerably increased by combining it with various compounds such as gold, platinum, carbon nanotubes, and so on [41–48]. The currentmetry of these biosensors is based on the performance of glucose oxidase (GOX) and electron exchange. In glucose oxidase, oxidation and reduction groups of Flavin Adenine Dinucleotide (FAD) are oxidized and reduced respectively, and hence it is necessary to establish a satisfactory electric relationship between the active location of FAD enzyme and the surface of electrode to have a current. Amperometric glucose biosensors mainly consist of stabilizing glucose oxidase in various media such as trapped polyacrylamide over working electrode surface. In the presence of glucose, oxygen, and enzyme, as the biological catalyst of this system, the following reaction is performed:

$$glucose + O_2 \xrightarrow{glucose-oxidase} glucuronic\ acid + H_2O_2 \quad (1)$$

The presence of enzyme causes the consumption of oxygen by glucose in the solution and reducing oxygen penetration to the auxiliary platinum electrode surface and leads to producing compounds such as glucuronic acid and hydrogen peroxide. Decomposition of hydrogen peroxide near the standard electrode (Ag/AgCl) produces two free electrons, as shown in Eq. (2), which is the main reason for the current. Until the enzyme is stabilized and there is enough oxygen, the relationship between the current and the concentration of glucose is linear [49].

$$H_2O_2 \xrightarrow{(Ag/AgCl)} O_2 + 2H^+ + 2e^- \quad (2)$$

Modification of the working electrode using nanoparticles with various sizes can improve the performance of biosensors, and increase the sensitivity and reduce the resistivity of the electrode in the route of electron exchange. These nanoparticles can be made from gold, silver, and zinc, which are widely used with various structures to modify the electric and

conductivity properties of electrodes [50–52]. Gold colloidal nanoparticles are metallic colloids and are used in various forms in the structure of the electrodes of biosensors. Using gold colloidal nanoparticles, the electric isolation effect is reduced in the protein cortex of glucose oxidase and electron exchange increases [53, 54]. The produced electron moves due to the effect of applying constant voltage on both sides of working and standard electrodes and this electron movement leads to an electric current which can be measured by ammeters. The amount of exchanged electron and/or the produced current indicates the amount of reacted glucose and its concentration in the sample [55]. In the current paper, the performance of two biosensors in completely identical conditions are compared while the only difference between them is the presence of gold colloidal nanoparticles in the electrode structure of one of them. These biosensors have different performances in similar currentmetry conditions and applying the gold colloidal nanoparticles leads to increasing the conductivity and improving the currentmetry.

Today, detecting the composition of foods through quality control tests is of great importance in food industries. High costs of traditional methods and the necessity for more accurate and sensitive measuring confirm the necessity of this issue. As a result, finding and/or improving faster, more accurate, more sensitive as well as cheaper measurement methods is always interesting for researchers and food producers [56–63].

The common analysis tools in food industries need skillful operators and are time consuming. These tools frequently need long separation time, costly equipment, and chemicals with high purity. A great part of these obstacles and problems can be removed by applying enzyme analyses. However, new food industries need to have small analysis tools to be used easily on non–solution samples and are able for simultaneous online control of one or more characteristics during production process or food processing. Most of these necessities can be acceptably met using enzyme electrodes, and hence improve the efficiency and optimization of the process and quality of products. Further, these enzyme electrodes should be cheap, reliable and strong, and they should have obvious preferences over the available methods [64–69].

One of the most important cause for cardiovascular diseases in recent years is high concentrations of cholesterol in blood. Cholesterol is found considerably in dairy products and yolk and its concentration can be determined using chromatography methods such as high performance liquid chromatography (HPLC) and gas chromatography (GC), which are of appropriate sensitivity and selectivity. However, applying fast and efficient methods is of great importance as these methods are time consuming and costly. Therefore, enzyme methods such as cholesterol esterase and cholesterol oxidase can be practically used as alternatives of traditional chromatography methods due to their simplicity, fast and effective [70–75].

Glucose is another important food component, which is frequently measured in quality control of food production processes. Until now, various spectroscopy methods, such as high performance liquid chromatography (HPLC), have been used for detecting glucose, especially in the fermentation process of nectars. However, enzyme methods are widely developed to do this [76–81].

The tendency of researchers in food industries for measuring these compounds with repeatability, selectivity, and high rate in very low concentrations in live environment leads to the development of tools called biosensors; and 85% of common biosensors is used for glucose measurement [82–87].

Generally, sensors are tools for detecting a chemical, physical and/or biological change and converting it to a measureable signal. A sensor includes a detector element, which is able to respond to the presence of a special analyte or a group of analytes. Another important part of a sensor is transducer that converts the created response into a sign. The third part of a sensor is signal processor which collects the received signal from transducer and, finally, after boosting it illustrates it.

Biosensors are a subset of chemical sensors, which have a completely especial performance in detecting biological processes. In this type of sensors, the detector elements are biological compounds such as proteins, enzymes, antibodies, nucleic acids, cells, tissues, and/or receivers which selectively react with the target analyte and create a response. This response is converted into an electrical signal in transducer and after processing the amount of this signal is illustrated as voltage, current, and/or impedance. The amount of this signal relates to the concentration of the analyte. Regarding the fact that the performance of biological detector elements is completely unique (for example, glucose oxidase only oxidizes glucose), biosensors make it possible to quantitatively evaluate and determine the concentration of an analyte, in addition to qualitatively evaluate the analyte and determine its presence or absence [88]. Figure 1 shows a schematic view of a biosensor.

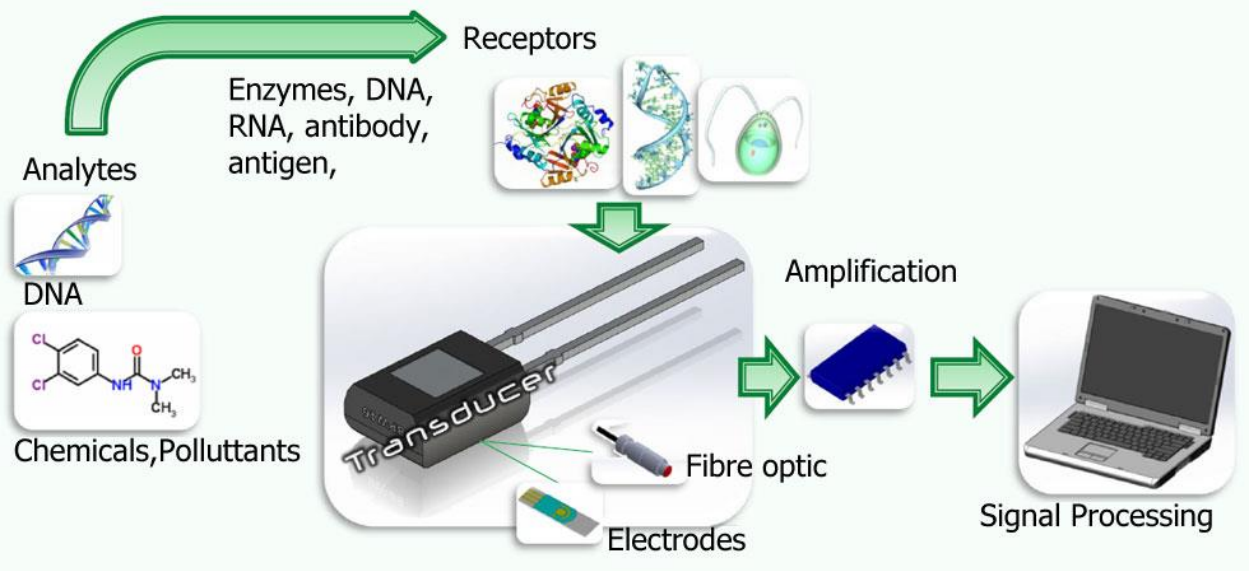

Figure 1. A schematic view of a biosensor.

The mentioned biological detector elements in aqueous solutions are of low durability on converter surfaces. For more durability, these materials should be stabilized over converter surfaces. Surficial absorption of these compounds with converter surface, trapping in a matrix during the covering of the converter surface with the matrix and creation of covalent bonds between the materials and converter surface is one of the methods used for this purpose. Trapping in matrix is the most effective and frequently used method. Matrices mainly include membranes, gel in carbon paste, graphite, silica, and/or polymer thin films. Undoubtedly, conductive polymer nanostructures–based matrices, especially polyaniline and polypyrole, are the most applicable and effective matrices due to high compatibility with biological components, ability for fast electron exchanging, considerably high effective area, and appropriate cohesion. In the current research, the application of polyaniline–based nanobiosensors for measuring glucose and cholesterol is discussed.

MATERIALS AND METHODS

In this study, three experimental steps were performed.

(i) Producing a gold plate covered with single–walled carbon nanotubes (SWCNT) and its preparation;

(ii) Preparing glucose oxidase for stabilization on the gold plate;

(iii) Stabilizing glucose oxidase using connective material PASE on the surface of carbon nanotubes and returning the activity of the enzyme.

Glucose (with 98% purity and molecular weight of 198.17 gr/mole), paraffin oil, dipotassium hydrogen phosphate (K_2HPO_4), and potassium hydrogen phosphate (KH_2PO_4) were supplied by Merck Co. for producing 0.1 M phosphate buffer. Glucose oxidase (35.5 Ku/mg) and gold colloidal nanoparticles (Au>48% and about 24 nm) were supplied by Sigma–Aldrich Corporation. Finally, carbon graphite powder (pure, mesh<325) was supplied by Sigma–Aldrich Corporation.

1. Producing Gold Plate Covered with Single–Walled Carbon Nanotubes (SWCNT) and Its Preparation

In this step, the following initial measures were performed for producing and preparing the gold plate:

1.1. Preparation of Gold Plate

In this step, a 10 mm ×10 mm gold plate with the thickness of 1 mm was produced and its surface was completely covered using precipitation with homological vapors (gold vapors) before any processing (Figure 2). The thickness of this homological layer was about 4–5 µm. Then, the surface of the gold plate was washed in two stages with concentrated sulfuric acid (H_2SO_4) and nitric acid (HNO_3), and finally with a large volume of deionized water for removing the remaining impurities and waste.

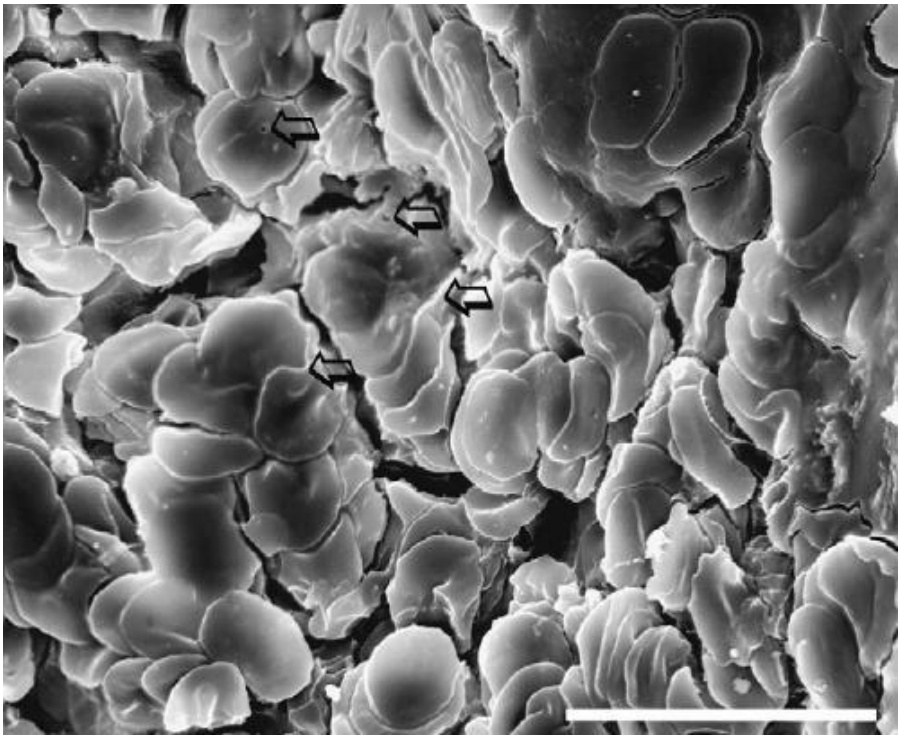

Figure 2. 10 mm × 10 mm gold plate with the thickness of 1 mm was produced and its surface was completely covered using precipitation with homological vapors (gold vapors) before any processing.

1.2. Deposition of Nickel Particle Catalyst

After preparing the gold plate, nickel catalyst was used for creating initial cores of carbon nanotubes and their regular growing up. The catalyst particles in the size of about 4 nm were deposited over the surface with medium regularity and density using lithography method. (This step has been performed in Nanotechnology Laboratory, California South University (CSU)) (Figure 3).

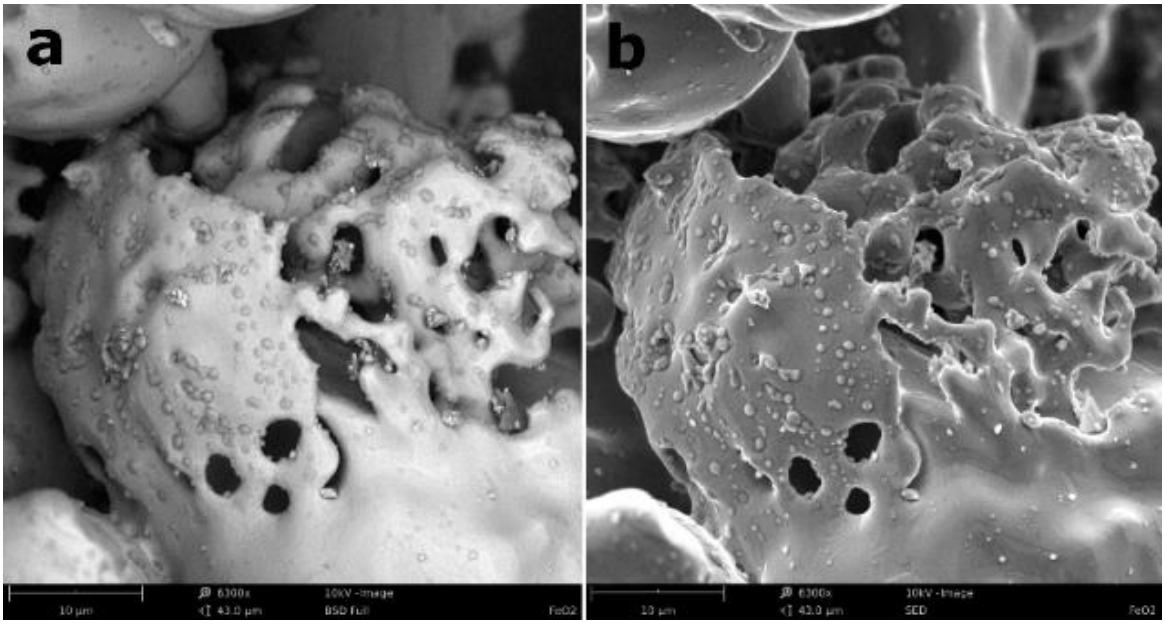

Figure 3. SEM images of the gold plate after catalyst particles in the size of about 4 nm were deposited over the surface with medium regularity and density using lithography method.

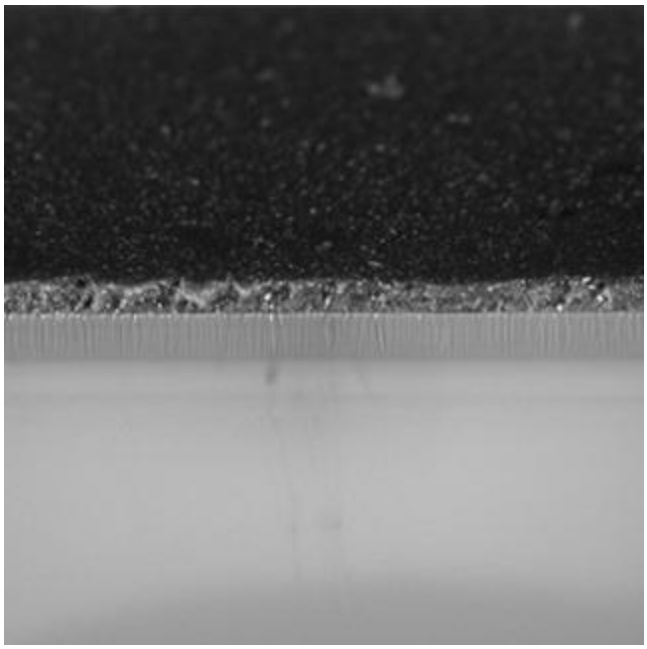

Figure 4. The developed nanotubes were single–walled with diameter of about 2–50 nm and height of 15–20 nm and developed vertically on the medium, according to scanning electron microscopy (SEM) images.

1.3. Development of Carbon Nanotubes (CNT)

For developing carbon nanotubes on the nickel nanoparticles stabilized on the gold plate, CVD method was used. In this method, the prepared gold plate was constantly placed into an oven under vacuum condition and light hydrocarbon (methane with a percent of butane) was pumped into the oven as gas. Due to the entering of this gaseous compound and chemical reactions in the oven, carbon precipitants emerged on the gold medium and regular carbon nanotubes were produced. The developed nanotubes were single–walled with diameter of about 2–50 nm and height of 15–20 nm and developed vertically on the medium, according to scanning electron microscopy (SEM) images. (This procedure was performed in California South University (CSU) Nanotechnology Research Institute in cooperation with some professors and experts) (Figure 4).

The area covered by these nanotubes was about 10–15 mm^2. Regarding the fact that each of these nanotubes acted as the base of sensor, it could be said that approximately 10^8–10^9 sensor bases were developed in the whole area of the gold medium (100 mm^2). This amount of density was very appropriate for stabilizing biological detectors.

For removing the remaining impurities and waste on the plate during the development process, the surface of the gold plate was washed in two stages with concentrated sulfuric acid (H_2SO_4) and nitric acid (HNO_3), and finally with a large volume of deionized water.

2. Preparing Glucose Oxidase for Stabilizing on the Gold Plate

Regarding high sensitivity of enzyme to environmental conditions and reaction situation and for maintaining active points of the enzyme until the end of operation and correct connection of the prepared enzyme on the surface of medium (developed nanotube), very important and accurate measures were performed and are mentioned in the following.

2.1. Preparing Glucose Oxidase Apoenzyme

For maintaining the active points of the enzyme until the end of operation, the active points of enzyme were firstly separated and a covering was placed over the enzyme. This process was performed using separation of flavin adenine dinucleotide (FAD) from the structure of the enzyme and preparing an apoenzyme. To perform this process, a saturated solution of $(NH_4)_2SO_4$ was firstly prepared and then its pH was decreased down to 1.4 at 20ºC using concentrated sulfuric acid (97% v/v). Glucose oxidase dissolved in phosphate buffer with the concentration of 20 mg/mL was added, drop by drop, during stirring to 20 mL of the saturated solution at 5ºC. This solution was maintained at this temperature for half an hour and then centrifuged for 15 minutes at 20000 rpm. The top yellow layer was separated from the compound after centrifuging (Figures 5a, 5b) and the

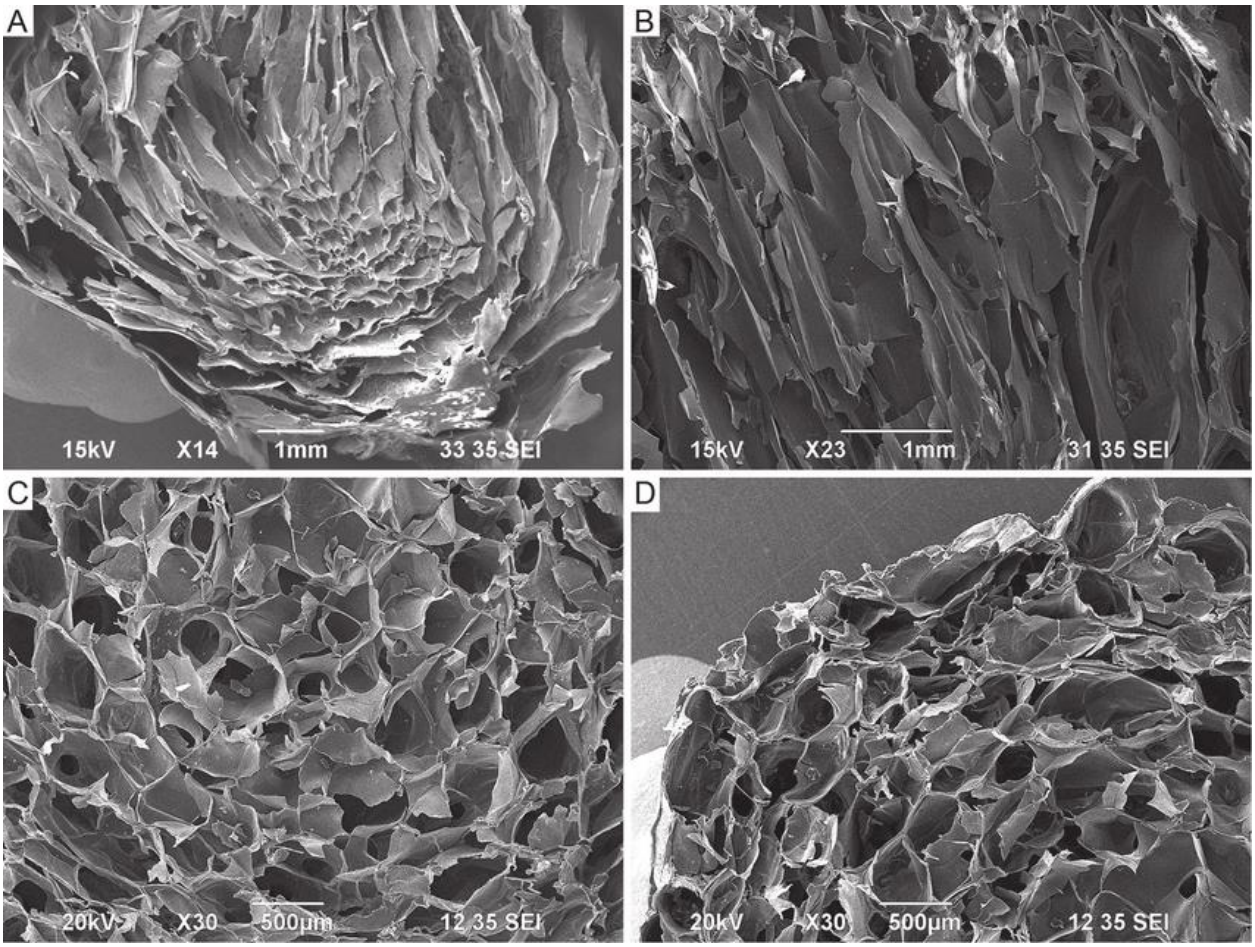

Figure 5. The top yellow layer was separated from the compound after centrifuging (a, b) and the obtained precipitant (c, d) was centrifuged in the same acidic pH condition twice and the obtained precipitant was collected.

obtained precipitant (Figures 5c, 5d) was centrifuged in the same acidic pH condition twice and the obtained precipitant was collected. The final precipitant was dissolved in phosphate buffer as the resource for glucose oxidase apoenzyme. (This step was performed in Research Center of Biotechnology, California South University (CSU)).

3. Stabilizing Glucose Oxidase Using Connective Material PASE on the Surface of Carbon Nanotubes (CNT) and Returning the Activity of Enzyme

After performing all the above mentioned steps, the enzyme and medium were separately prepared for stabilizing. Regarding the fact that a gold electrode was used in this study and direct contact of enzyme and metal changes the natural structure of the enzyme, the medium surface was covered with a layer of cystamine.

Mainly, protein was added to the single layer of cystamine in these processes for sensor manufacturing. Therefore, it was positively charged. As a result, it could create an electrostatic absorption with the negatively charged enzyme. Hence, the relationship between the enzyme and medium facilitates [89–97].

For stabilizing glucose oxidase on the developed carbon nanotubes on the gold plate, pyrenebutanoic acid succinimidyl ester (PASE) was used in this study as the connective material, which has a pyrene group for making Van der Waals bonds with the carbon nanotubes and an amid group for connecting to the enzyme [98–127].

For accurate stabilization, the prepared medium was firstly stirred in a solution of the connective material at the concentration of 2.3 mg/mL and DMF, and after 2 hours the medium was exited from the solution and washed with pure DMF, and at the same time the prepared apoenzyme was dissolved in screened and deionized water with the concentration of 10 mg/mL.

Then, the washed medium was contacted to the apoenzyme solution for 18 hours and, finally, the medium was washed with very clear water for 6 times to

remove all impurities produced during the process.

3.1. Returning the Activity of Stabilized Enzyme on the Medium

Regarding the fact that the enzyme was changed to apo for protecting against loss of enzyme activity during stabilization steps, it was necessary to activate the enzyme by returning the removed FAD molecule to the structure of the enzyme after the stabilization process.

To perform this step, 200 µM of FAD molecules obtained from changing the enzyme to the apoenzyme was incubated for 1 hour in 0.1 M phosphate buffer with the concentration of 150 µg/mL and at pH 6 at room temperature. This process formed the stable complex of FAD protein which in fact was reconstructed enzyme. Its separation constant was very small (k<10M) and could be very effective for returning enzyme activity.

3.2. Investigating the Activity of Stabilized Enzyme on the Medium

After performing the stabilizing operation, enzyme activity of the incubated mixture was measured in the following form after placing at room temperature for 30 minutes to determine and confirm the returning of the enzyme activity.

In this method, the prepared medium was placed in a solution containing potassium phosphate measuring buffer (measuring buffer was prepared by dissolving 0.1 ml of 1% o–Dianisidine indicator in 12 ml of phosphate buffer with the concentration of 0.1 M and at pH 6.0), 10 µL of 18% glucose (in water), 10 µL of peroxidase with the concentration of 200 µg/mL and 10 µL of glucose oxidase (dilution of 200 times) with the concentration of 1 mg/mL, and the absorbance at the wavelength of 460 nm at various times was measured by JENWAY 6305 spectroscope (available in Laboratory of Microbiology, California South University (CSU)) (Figure 6). (Absorption value indicates the amount of glucose consumed by the enzyme and hence enzyme activity [100, 108]).

4. Electrode Preparation

Firstly, carbon graphite powder was placed into an oven for 30 minutes in 700ºC so that volatile and absorptive materials were removed from the graphite powder and surface activity increased. Then, it was place in a desiccator for1 hour. This powder was the raw

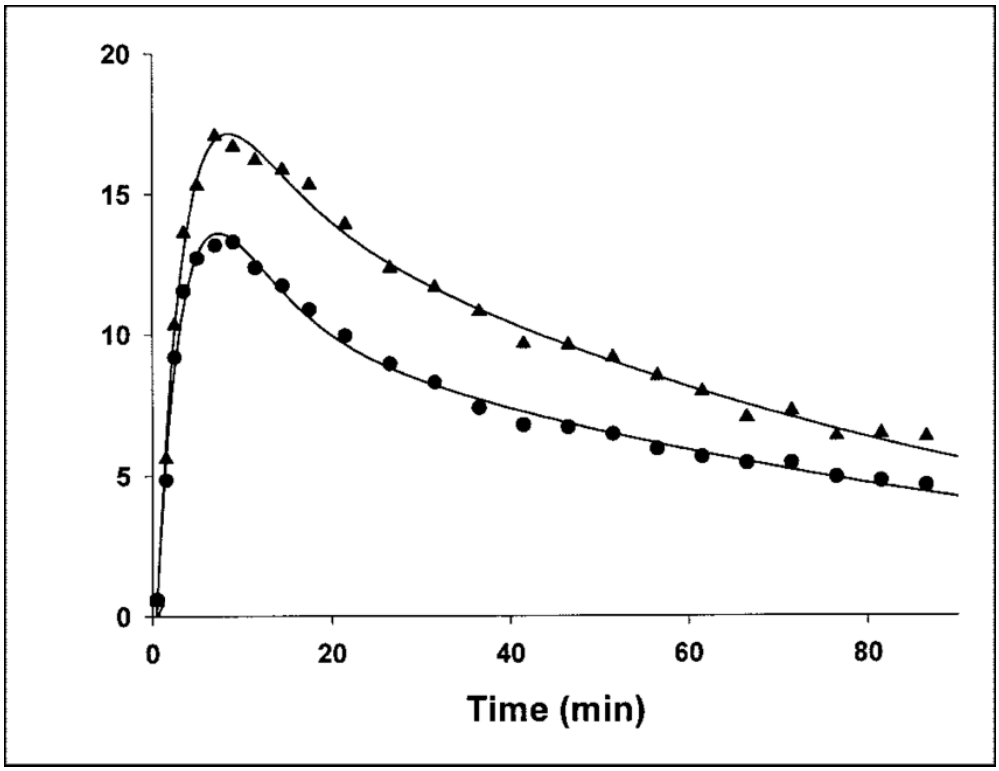

Figure 6: Enzyme activity before (lower curve) and after (upper curve) stabilizing operation process according against time which showed stable and activation of the enzyme after stabilizing.

material for producing the electrode. CP (Carbon Paste) was produced by adding 100 mg of carbon graphite powder to 36 µ) of paraffin oil, according to [128–163]. The modified CP with gold colloidal nanoparticles was produced by adding 300 µl of gold colloidal nanoparticles to 100 mg of carbon graphite powder and after evaporation of water in a desiccator for 3 hours, 36 µl of paraffin oil was added to it. By inserting these mixtures, separately, in glass tubes with an internal diameter of 4 mm, CPE electrode and Au_{nano}/CPE were prepared and the electrical connection with an ammeter was established through copper wires placed into the electrodes. When these electrodes were not in use, they were kept at 4ºC.

5. Enzyme Preparation and Biosensor Production

Oxidation of glucose by glucose oxidase and production of glucuronic acid reduced the pH of the reaction environment. To prohibit severe variations of the pH and maintain the activity of the enzyme, a specified amount of the enzyme was placed into phosphate buffer. To prepare 0.1 M phosphate buffer, K_2HPO_4 and KH_2PO_4 were used and the pH was adjusted with H_3PO_4 and NaOH.10 mg of glucose oxidase was added to 1 ml of 0.1 M phosphate buffer (PBS) in semi–permeable membranes and a membrane was fastened around each CPE electrode and Au_{nano}/CPE. Then, the produced biosensors were placed into glucose solutions with the concentration range of 0–1 mM for currentmetry.

6. Conductive Polymers

Conductive polymers are a type of organic materials which have electric conductivity. It seems that metals have electrical conductivity and organic materials are dielectric, while conductive polymers are of both properties. Another advantage of conductive polymers is their process ability, i.e., their ability to be dissolved or melted.

These characteristics cause these polymers to be produced and used in various forms. In addition, these polymers are flexible due to their plastic nature. Further, their electric conductivity can be set [164–207].

The reason for their electric conductivity is their coupled bond structure. It means that the presented molecules in π bonds of these structures can be moved along the polymerization chain and conduct electric current. Figure 7 shows the coupled structure of some conductive polymers.

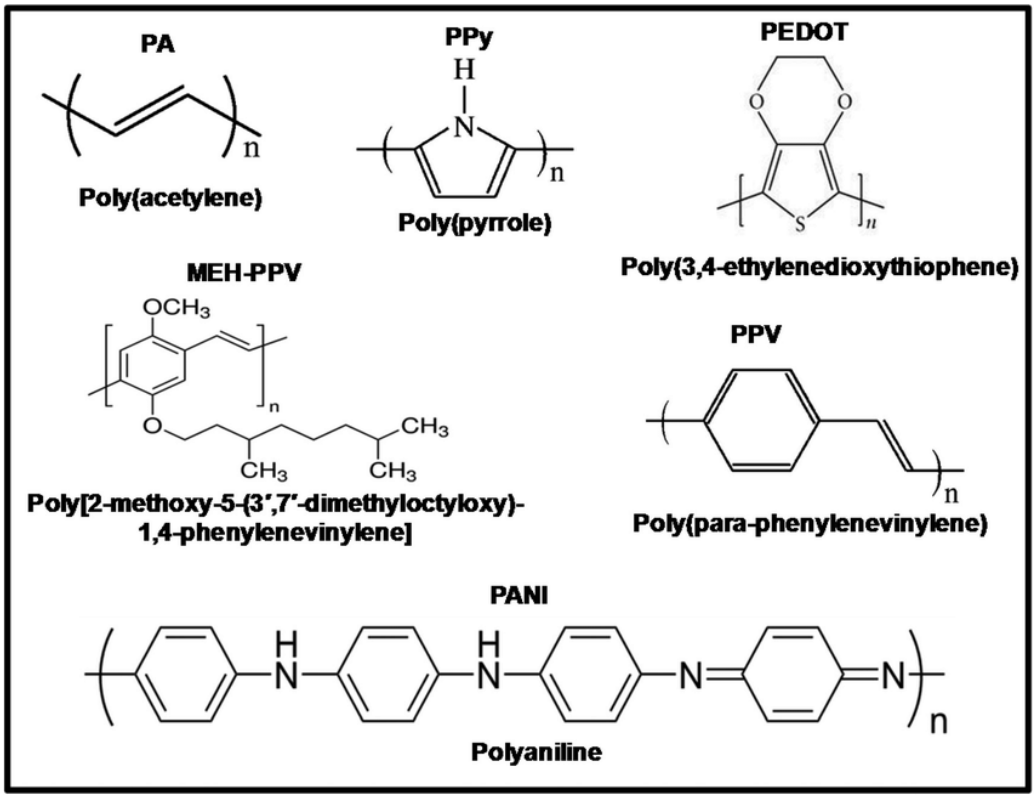

Figure 7. Coupled structures of some conductive polymers.

Among conductive polymers, polyaniline has been more interesting for researchers than others due to its high electrical conductivity, simple production process, good environmental stability, and unique chemical nature (oxidization/reduction). The previously performed studies in recent years on the production polyaniline in nano scale caused the improvement of the most interesting property of this polymer, namely the electrical conductivity. In addition, increasing the effective area of the polymer leads to improvement of its process ability, and hence application of this polymer increase in various sciences, especially food industries [208–243]. Up to now, various types of polyaniline nanostructures have been produced such as nanoparticles, nanofibers, nanotubes, nanowires, nanorods, and nanobolts.

The above mentioned properties of the conductive polymer nanostructures cause these materials to be considered as the most interesting options for the stabilizing matrix of biodetector elements on the transducer of biosensors. Among the produced nanostructures from polyaniline, nanoparticles, nanofibers, and nanotubes of this material have been used in biosensors [244–288].

In the following sections, applications of these materials in the structure of biosensors as well as the methods used for measuring sugars, proteins, and fats using these materials are discussed.

7. Biosensors

As previously mentioned, biosensors are a type of sensors which have an amazing, unique performance in the presence of intervening factors. Stabilizing each bio-operator on the transducer of biosensors leads to creation of a completely unique response to that analyte. Hence, biosensors are amazing tools from selectivity point of view.

Generally, analyte–biodetector element interaction in a biosensor causes to creation of a change in a parameter. This change is converts into an electrical signal by transducer and after processing, is illustrated [289–303].

7.1. Bioelement Stabilizing Methods

Till now, various physical and chemical methods have been proposed for stabilizing bioelements. However, they should be stabilized so that their active locations are not blocked and their geometrical forms have not changed. In addition, it is necessary to have a relationship between biodetector element and sensitive area of transducer [304–317].

Trapping the enzyme in a matrix, e.g., an electropolymer film, is one of the most frequently used methods for stabilizing the enzyme. Another method is creating a covalent bond between protein and transducer surface, in which detector element is very high. These connections are established through functional groups of detector element such as SH, OH, COOH, and NH_2, which are not necessary for biological reaction.

Surficial absorption is another method that is based on gravitational force between detector element and transducer surface and is used to stabilize detector elements. Lifespan of biosensor prepared by this method is very short. However, surficial absorption is very simple since it has no need to any other reagent and failure of the enzyme is limited. Connecting the biological detector elements through electrostatic absorbers is another method for stabilizing these compounds. In this method, positive or negative charges are induced on transducer surface by applying a potential and then biological detector element is absorbed by the surface through electrical induction. Figure 8 shows six most common types of methods used for stabilizing biosensor elements.

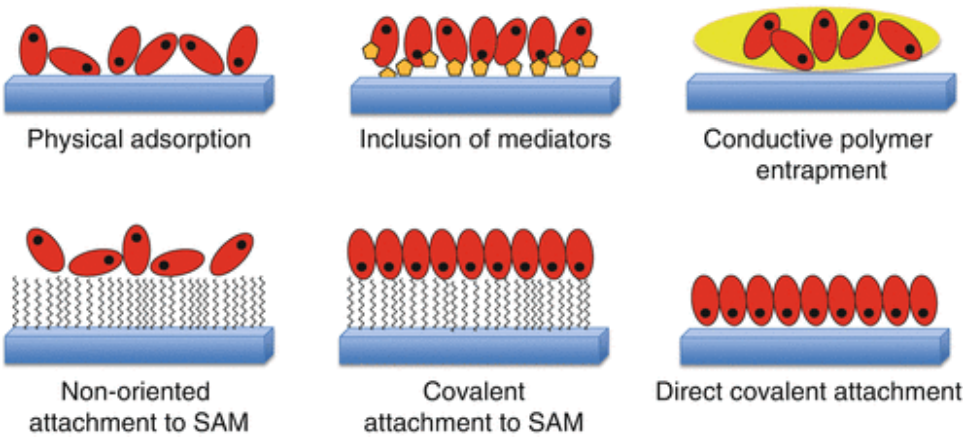

Figure 8: Six most common types of methods used for stabilizing biosensor elements.

Conductive polymer nanostructures can be used as stabilizers of biodetector elements due to their electrical conductivity, compatibility with live materials, environmental stability, and high contact surface.

8. Cyclic Voltammetry

Cyclic voltammetry is an electrochemical method for detecting the presence of operational electroactive components, which are able to exchange electrons in an electrochemical reaction in an aqueous environment, in a solution. Since the working process of the considered biosensors is based on an electrochemical reaction, cyclic voltammetry is an appropriate method for detecting the presence of an analyte in solution. In this regard, transducer of a biosensor is used in this method as working electrode. In this method, working, auxiliary, and standard electrodes are used. Standard electrode is of constant potential in various currents. Usually, silver/chloride standard electrode is used. Auxiliary electrode is usually made from typical platinum and working electrode includes transducer and polymer cover containing detector element.

After placing these three electrodes in the solution, a potential range between two specified values is cyclically applied to working and standard electrodes and the currents obtained from working and auxiliary electrodes are illustrated in terms of the applied potential. Therefore, a current against potential curve can be obtained. In this graph, current increases when potential reaches a value in which an electroactive type can be oxidized and hence a peak emerges in cyclic voltammetry graph.

When potential scanning is applied in the opposite direction, i.e., from higher values to lower ones, electroactive types with ability for reduction are reduced and create a peak in the current. Since each material has its own specific potential (oxidization–reduction), analyte can be detected through this method [318–339]. As a result, cyclic voltammetry method is used as the most important test for performance of transducer and sensor zone of biosensors. Figure 9 shows a schematic view of cyclic voltammetry device, potential application, and the obtained cyclic voltammetry graph.

9. Glucose Detection

In biosensors used for detecting glucose, the reactions performed on the bioelectrode (working electrode) are in the following forms:

$$glucose \xrightarrow{GOX} C_6H_{10}O_6 + H_2O_2 \quad (3)$$

$$H_2O_2 \rightarrow H_2 + O_2 + 2e^- \quad (4)$$

Heidari *et al.* [340–355] investigated the biosensors that were used for detecting glucose based on glucose oxidase stabilizing in polyaniline nanowires. In this method, aniline monomers were firstly polymerized in a product containing ammonium peroxide disulphate as oxidizer and then they were precipitated on a carbon

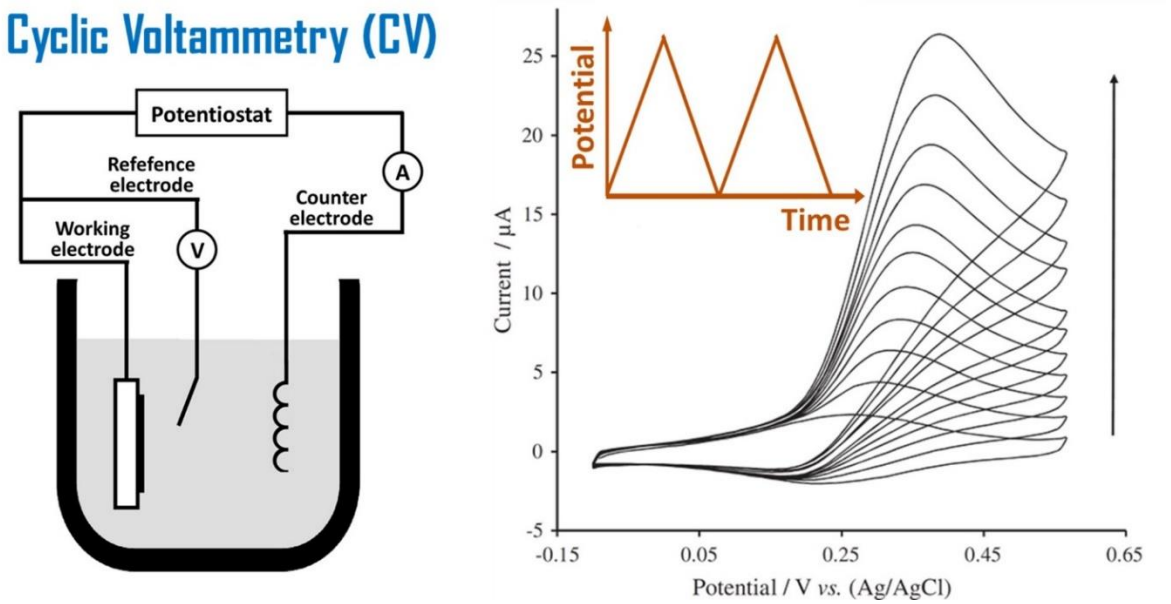

Figure 9. A schematic view of cyclic voltammetry device, potential application and the obtained cyclic voltammetry graph.

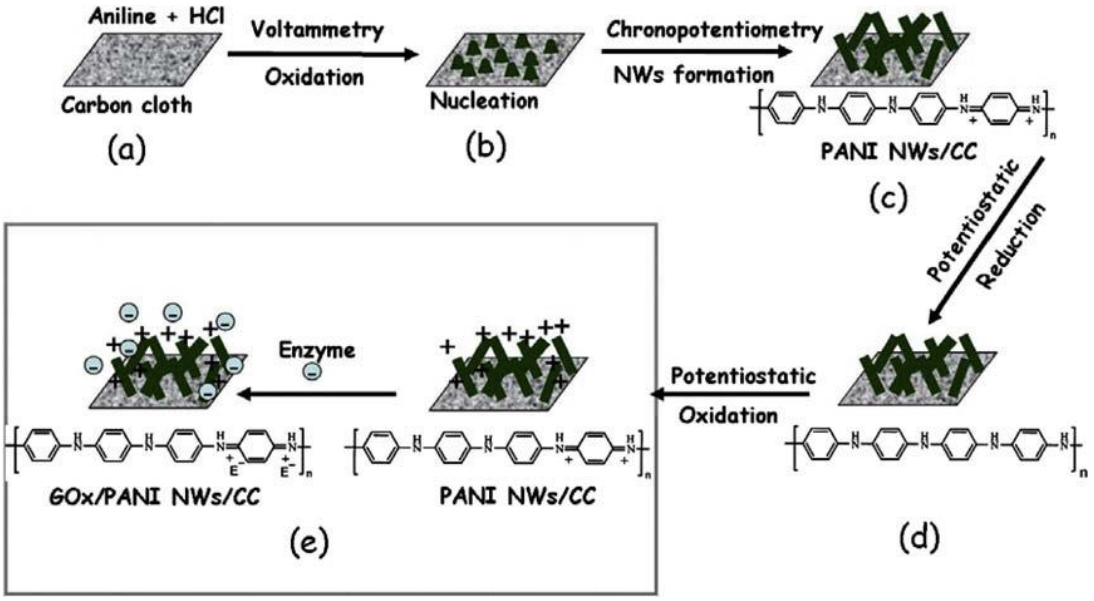

Figure 10. A schematic view of positive charges cause electrostatic absorption of glucose oxidase induced from negative surface charges.

electrode as a film. When polyaniline particles were growing, polymerization of aniline continued by applying a potential. Then, polyaniline nanowires were produced by applying a constant current to the carbon electrode. Afterwards, this electrode was placed in a phosphate buffer solution (pH=7.2) and polyaniline nanowires reduced by applying a constant potential. This caused anions to be removed from the surface of polyaniline and the appropriate conditions for surface absorbing of glucose oxidase were prepared. Then, the electrode was placed in a phosphate buffer solution containing 2.5 mg/l glucose oxidase, and by applying 0.25 V, positive charges were induced on polyaniline nanowires. These positive charges caused electrostatic absorption of glucose oxidase induced from negative surface charges. Figure 10 schematically shows this process. In order to investigate the performance of the produced electrode, cyclic voltammetry technique was

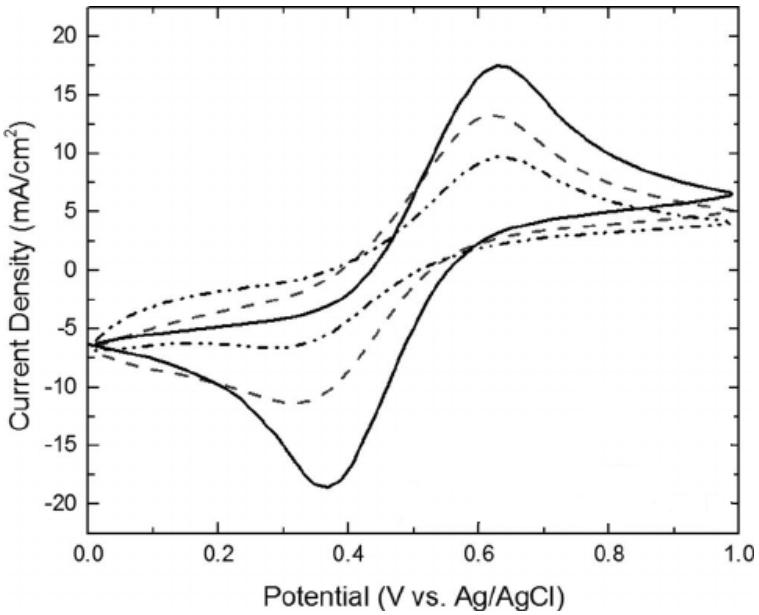

Figure 11. When glucose oxidase is in a stable state, the related oxide peaks emerge, while when there is not enzyme, oxide peaks do not emerge.

used. The produced electrode was placed in solutions with and without glucose. The resulting voltammetry graph showed that when glucose oxidase was in a stable state, the related oxide peaks emerged while when there is not enzyme, oxide peaks did not emerge (Figure 11). This observation was performed for evaluating the correct performance of biosensors.

Another study was performed by Heidari *et al.* [356–360] about the stabilizing of glucose oxidase with polyaniline nanotubes. In this study, a membrane of aluminium anodic oxidation with outer diameter of holes between 200 and 250 nm, and inner diameter of holes equal to 100 nm was used to synthesize polyaniline nanotubes.

Firstly, one side of aluminum anodic oxidation was covered with 10 nm thick platinum layer through evaporation in vacuum. Then, a copper wire was connected to the platinum layer for conducting electric current. After isolating the copper wire and backside of platinum to prohibit incident contact with the solution containing the sample, the produced electrode was placed in a solution containing 0.5 M sulfuric acid and 0.2 M aniline monomers. By applying scanning potential, aniline polymerization and polyaniline precipitation in holes of aluminum anodic oxidation were performed and polyaniline nanotubes were produced.

In order to stabilize glucose oxidase, polyaniline nanotubes were reduced in phosphate buffer solution through applying 250 mV so that the anions around the polyaniline nanotubes were removed. Then, polyaniline nanotubes were oxidized in phosphate buffer solution containing 7 mg/l glucose oxidase under 750 mV to electrostatically absorb glucose–oxidase. During oxidation, glucose oxidase, which was negatively charged, absorbed onto the inner walls of polyaniline nanotubes and became trapped. Then, the electrode was washed with distilled water to remove enzymes that were not appropriately absorbed by the inner walls of the nanotubes.

In order to investigate the performance of the produced electrode, cyclic voltammetry technique was used.

10. Cholesterol Detection

In biosensors used for detecting cholesterol, the reactions performed on the bioelectrodes are in the following forms:

$$cholesterol + O_2 \rightarrow cholesterol - ten - 30ne + H_2O_2 \quad (5)$$

$$H_2O_2 \rightarrow 2H^+ + O_2 + 2e^- \quad (6)$$

Heidari *et al.* [356–360] used polyaniline nanotubes for stabilizing lipase on biosensors used for detecting cholesterol. In this method, as can be seen in Figure 12, polyaniline nanotubes (PANI–NT) were firstly produced through chemical polymerization reaction. Then, these nanotubes were precipitated on the surface of indium–tin oxide electrode by electrophoretic method as a film. Then, the produced electrode was placed into a solution containing glutaraldehyde (GLU). The reason for using glutaraldehyde is that this compound has a carbonyl group at both ends. It can bond with nitrogen of polyaniline film on the surface of indium–tin oxide from one end and connects to nitrogen groups of lipase at the other end. Therefore, lipase stabilized on the polyaniline film covalently. After connecting glutaraldehyde to the film surface, electrode dries and enters to lipase solution and after sometime electrode dries.

In this investigation, the performance of the produced electrodes was evaluated by cyclic voltammetry. In this study, three types of electrodes, ((PANI–NT)/ITO) (electrode covered with carbon nanotubes without glutaraldehyde and/or lipase), (PANI/GLU/ITO), and ((LIP/GLU/PANI)–(NI–ITO)) were compared in environments with and without cholesterol. Observing the peaks related to the reaction of lipase and cholesterol available in the sample container for electrode and their disappearance in two other states confirmed the correct performance of the electrodes.

In a similar study, Heidari *et al.* [360–368] produced biosensors for detecting cholesterol based on polyaniline film covered on an electrode of indium–tin oxide by electrochemical method.

In this study, polyaniline was firstly covered on an electrode of indium–tin oxide by electrochemical polymerization and then all steps performed by Heidari *et al.* were repeated.

In another investigation, Heidari *et al.* [360–368] produced cholesterol biosensors through simultaneously stabilizing cholesterol oxidase and cholesterol esterase on polyaniline film. In this method, polyaniline was firstly covered on an electrode of indium–tin) oxide through electrochemical polymerization [369–381]. Then, 1% glutaraldehyde was distributed over the polyaniline film and the surface was allowed to dry. Then, cholesterol esterase was distributed over the dried surface of electrode and after it dried, cholesterol oxidase was distributed and dried. Then, this (enzyme–polymeric) set was washed with distilled water to remove oligomers and not stabilized enzymes. The results obtained from cyclic voltammetry confirmed the presence of cholesterol and cholesterol oleate.

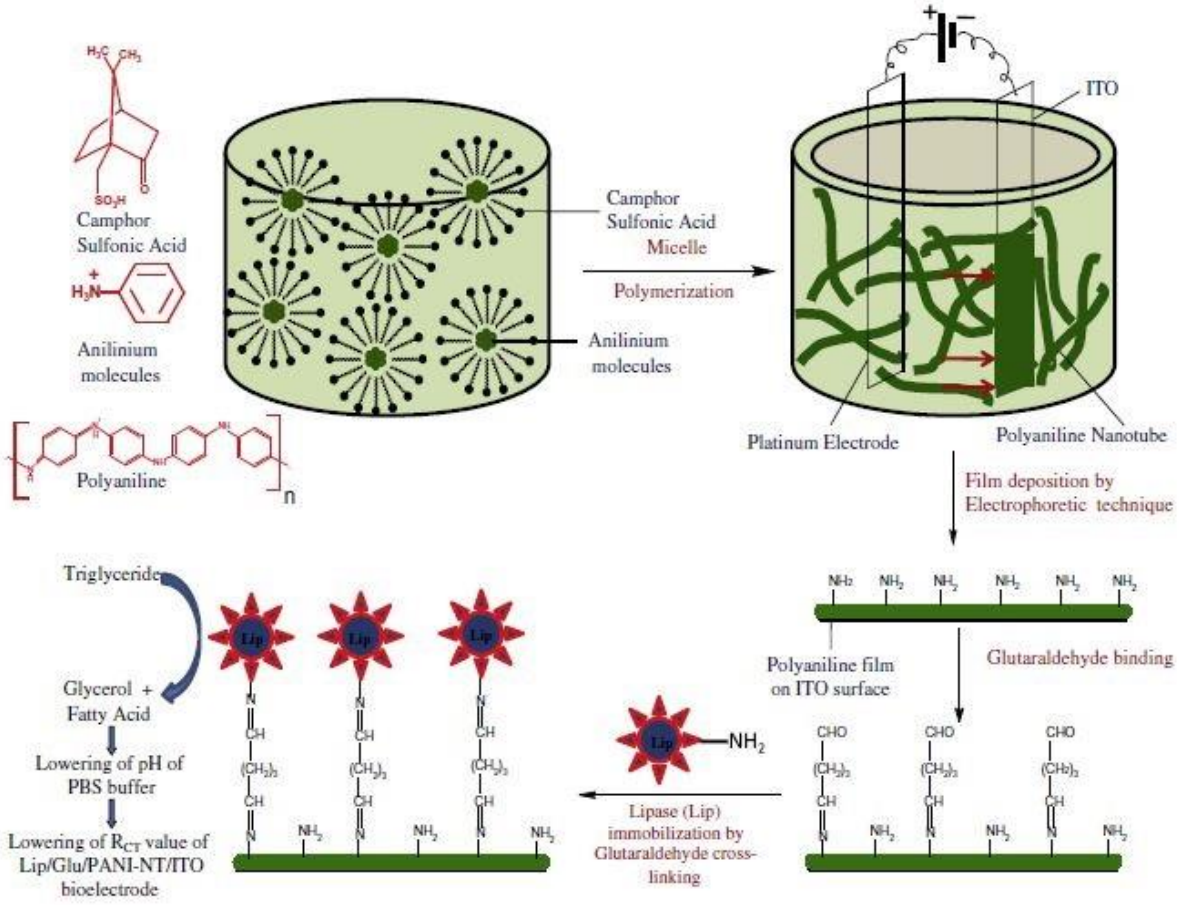

Figure 12. Usage polyaniline nanotubes for stabilizing lipase in biosensors used for detecting cholesterol. Polyaniline nanotubes (PANI–NT) were firstly produced through chemical polymerization reaction.

RESULTS AND DISCUSSION

1. Currentmetry

Currentmetry of the biosensors was performed separately through standard (Ag/AgCl), CPE, and (Au_{nano}/CPE) electrodes at room temperature. Glucose solutions with specified concentrations were prepared for currentmetry of the biosensors and the produced current was measured by ammeters by applying the same potential, 0.7 V to both biosensors.

Figure 13 shows the currentmetry of the biosensors in terms of glucose concentration with different performances of CPE and (Au_{nano}/CPE) electrodes. The curves showed that the concentration of substrate (glucose) affects the activity of glucose oxidase. In very low concentrations of substrate, not all active locations of the enzyme were filled with the substrate and the activity of the enzyme would be low. By gradually increasing the concentration of the substrate, enzyme activity increased until reaching to a specified concentration in which all active locations of the enzyme were filled with the substrate and enzyme activity reached its maximum amount under operational conditions. In Figure 13, curve b (performance of (Au_{nano}/CPE) electrode) is of higher currents than curve a (performance of CPE electrode) due to the presence of gold colloidal nanoparticles. The maximum current response of CPE and (Au_{nano}/CPE) electrodes in phosphate buffer at pH=4 were 0.4 and 1.2 µA, respectively, which showed different performances of the two electrodes at similar potential and pH. In Figure 14, currentmetry of the biosensors in terms of the concentration of glucose is shown for two different performances of CPE and (Au_{nano}/CPE) electrodes. In Figure 14, the upper curve (performance of (Au_{nano}/CPE) electrode) is of higher currents than the lower curve (performance of CPE electrode) due to the presence of gold colloidal nanoparticles.

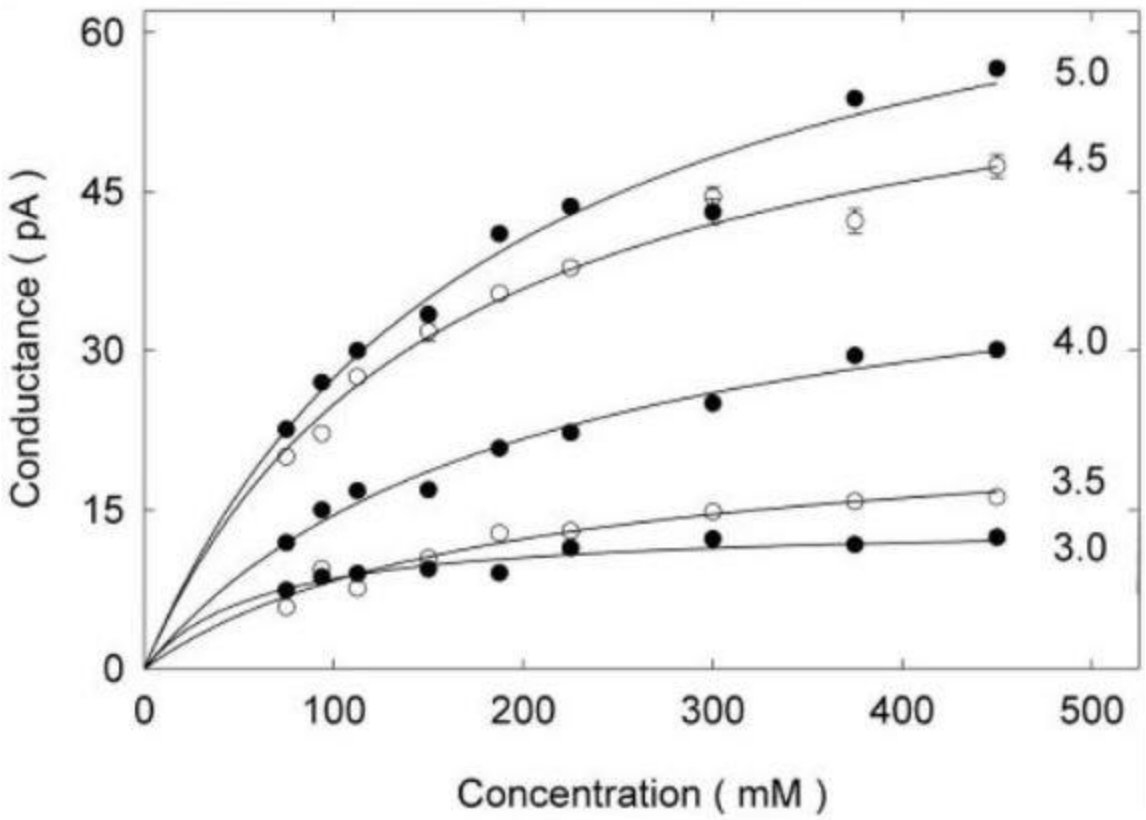

Figure 13. Currentmetry of biosensors in terms of glucose concentration with different performances of CPE and (Au_{nano}/CPE) electrodes.

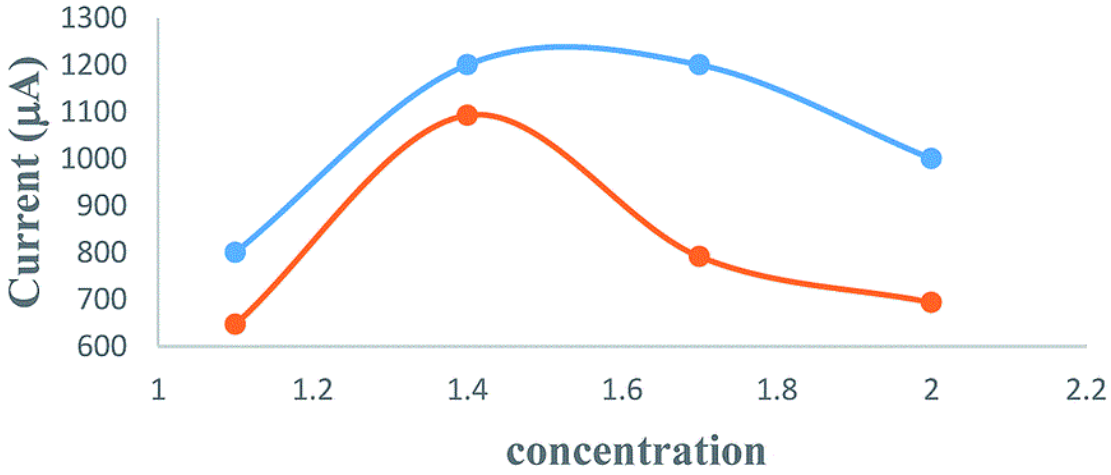

Figure 14. Currentmetry of biosensors in terms of the concentration of glucose shown for two different performances of CPE and (Au_{nano}/CPE) electrodes. In this figure, the upper curve (performance of (Au_{nano}/CPE) electrode) is of higher currents than the lower curve (performance of CPE electrode) due to the presence of gold colloidal nanoparticles. It should be noted that x–axis and y–axis show concentration (pH) and current (µA), respectively.

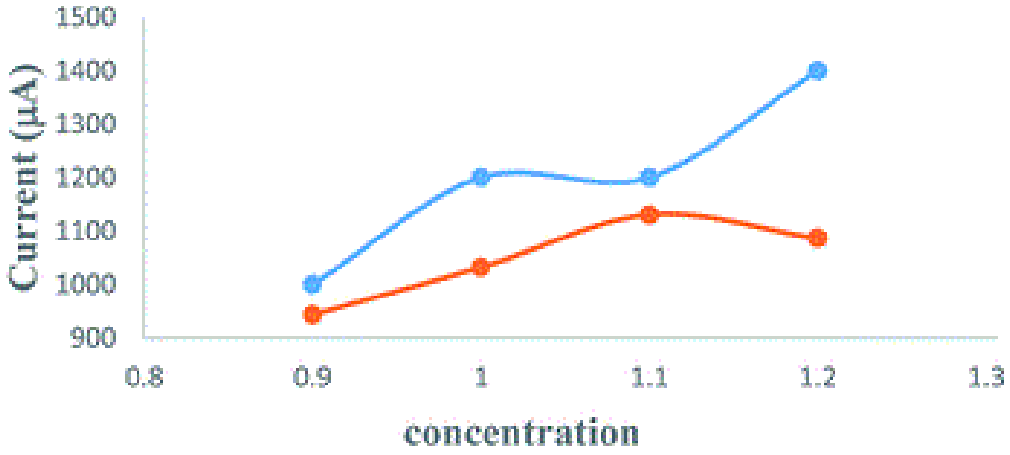

Figure 15. The maximum current response of CPE and (Au_{nano}/CPE) electrodes in phosphate buffer at pH=6 was 0.7 and 1.58 µA, respectively, which showed considerable different performance of the two electrodes in similar potential and pH. It should be noted that x–axis and y–axis show concentration (pH) and current (µA), respectively.

In addition, according to Figure 15, the maximum current response of CPE and (Au_{nano}/CPE) electrodes in phosphate buffer at pH=1.1 was 1100 µA and at pH=1.2 was 1400 µA, respectively, which showed considerably different performance of the two electrodes in similar potential and pH.

In Figure 16, currentmetry of the biosensors in terms of the concentration of glucose is shown for two different performances of CPE and (Au_{nano}/CPE) electrodes. According to Figure 16, the maximum current response of CPE and (Au_{nano}/CPE) electrodes in phosphate buffer at pH=13.78 was 1450 µA and at pH= 13.76 was 1550 µA, respectively. In this figure, curve b (performance of (Au_{nano}/CPE) electrode) is of higher currents than curve a (performance of CPE electrode) due to the presence of gold colloidal nanoparticles. It means that carbon electrode modified with gold colloidal nanoparticles prepares appropriate environment for direct movement of electrons due to high electrocatalystic activity of nanoparticles, hence leads to facilitation of electron movement, higher currents, and. finally, better tracing of glucose due to higher conductivity. By evaluating these currentmetries, the positive effect of gold colloidal nanoparticles is confirmed and (Au_{nano}/CPE) electrode is selected as the appropriate electrode.

Using Figure 16 and comparing the illustrated graphs for various concentrations in variation of pH against current, it can be seen that maximum current was achieved at pH=13.76 and increasing the concentration of glucose led to producing higher ampere. It indicates that optimum condition was achieved, in which current was maximum and the amount of detected glucose was maximum.

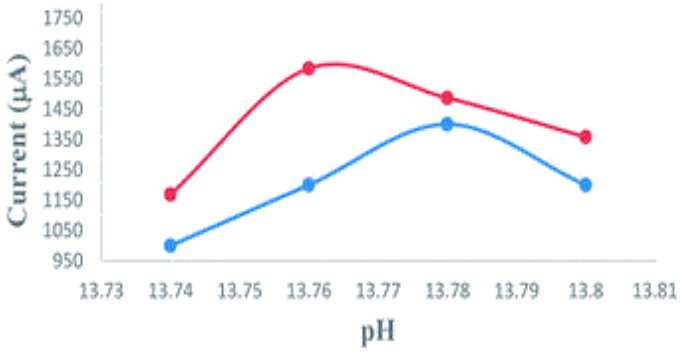

Figure 16. Currentmetry of biosensors in terms of the concentration of glucose is shown for two different performances of CPE and (Au_{nano}/CPE) electrodes. It should be noted that x–axis and y–axis show concentration (pH) and current (µA), respectively.

CONCLUSION

After completing the experimental steps, the nano medium was produced. This medium can be used as high accurate and sensitive nano–biosensor due to the stabilized enzyme on its surface.

For protecting enzyme activity from devastating effects of metal media during stabilization processes, it is necessary to cover the medium surface with an appropriate material such as cystamine.

Removing the active points of enzyme (making apo) before the start of stabilization step is necessary for protecting the performance of the enzyme.

Regarding the relatively large size of glucose oxidase, this enzyme should be connected to the outer wall of the carbon nanotube using a connective material such as 1–pyrenebutanoic acid succinimidyl ester (PASE).

Regarding the fact that the medium was placed into phosphate buffer and accurately washed after each measuring of activity, the possibility of the presence of free (non–stabilized) enzymes on the medium was very low and it could be assuredly said that the measured activity of about 280 u/mg shown initially in Figure 6 was only due to stabilized enzymes and it confirmed that temporary removing of enzyme activity and returning its activity after completing the stabilizing steps cannot permanently inactivate enzymes although it can remove some enzymes from their third structure.

As can be seen in Figure 6, the variation of the activity of the stabilized enzyme against time did not considerably change compared to the activity of the free enzyme. It confirms the stability of the stabilized enzyme.

Creating medium density (mentioned in the paper) in developed nanotubes affects the penetration of enzyme and its stability.

Regarding the operational level, high conductivity, and flexibility of carbon nanotubes compared to other metals, they are appropriate for stabilizing various chemical and biological detectors and utilizing them in manufacturing biosensors leads to increasing efficiency and sensitivity, and decreasing resistivity in performance.

In this study, glucose oxidase biosensor was experimentally manufactured using carbon nanotubes based on the investigations in various previously performed researches in this field. Although these tests were performed similar to experimental studies in some steps, obtaining new results such as temporary inactivation of the enzyme and using gold plate, alone, in macro plate form as the medium were the differences of the current research with similar researches.

Although the performed studies in the field are in the level of initial manufacturing of these sensors, it leads to preparing an appropriate space for performing more developed research works in this field. Experimental researches performed in this study and the obtained results can be represented to researchers with this aim. Hopefully, more acceptable results will be achieved if more applicable plans will define.

Evaluations of the performance of biosensors with two different electrodes showed that enzyme activity was low at very low concentrations of glucose for both biosensors. Then, by gradually increasing glucose concentration, enzyme activity increased until reaching a specified concentration at which all active locations of the enzyme were filled with substrate and enzyme activity reached to its maximum capacity. The results obtained from currentmetry of the biosensors showed that by increasing the concentration of glucose and after reaching a specific amount, enzyme activity reached a stage at which its rate did not change with the increasing glucose concentration and remained constant. This phenomenon happened when all active locations of the enzyme were occupied and there was not enough active space for oxidizing the available glucose. To maintain the activity of active points of glucose oxidase, the enzyme was placed in phosphate buffer so that pH of the reaction environment was controls using the buffer and enzyme activity was maintained during oxidization. Investigation of the performance of the biosensors at various pH values of phosphate buffer showed that enzyme activity and currentmetry of both biosensors in phosphate buffer at pH=6 increased. This increasing in the activity was due to creation of an appropriate ionic state for substrate and/or glucose oxidase. Oxidation and reduction groups in glucose oxidase, which were oxidized and reduced, were deeply deposited in holes and so they were not easily available for guiding electrons towards electrode surface and this was against the performance of the enzyme. Therefore, in establishing the current, it was necessary to prepare satisfactory electric relationship between active locations of the enzyme (FAD) and surface of the electrode. To solve this problem, gold colloidal nanoparticles were used in the structure of (Au_{nano}/CPE) electrode. It led to the increase in the conductivity, facilitating the movement of electrons, and increasing the satisfactory electric relationship between electrode surface and active locations of the enzyme (FAD). Modification of (Au_{nano}/CPE) electrode with gold colloidal nanoparticles led to creation of a micro-environment like oxidization–reduction of proteins,

which was due to high electrocatalystic activity of the nanoparticles. It meant that the isolation effect in protein cortex of the enzyme was reduced and electron exchange was increased. Another reason for using gold colloidal nanoparticles in the structure of (Au_{nano}/CPE) electrode was its high sensitivity and selection ability, increasing the electric conductivity and permeability between biological fences (enzyme–electrode) and it considerably improved glucose tracing by the biosensors.

Detecting glucose and cholesterol in quality control tests of food production processes are very important. Although these methods should be fast, accurate, sensitive, and cheap, the current methods need skillful operators and are time consuming. To solve this problem, one type of chemical sensors, called biosensors that are of unique performances, can be used. Conductive polymers–based biosensors, especially aniline polymers are greatly interesting for researchers due to their unique properties such as high electric conductivity, large contact area, and simple preparation method. The appropriate performance of these biosensors introduces them as the most important measurement tools to the market.

REFERENCES

1. Heidari, A., Brown, C. (2015) Study of composition and morphology of cadmium oxide (CdO) nanoparticles for eliminating cancer cells, *J Nanomed Res.*, **2(5)**, 1–20.

2. Heidari, A., Brown, C. (2015) Study of surface morphological, phytochemical and structural characteristics of rhodium (III) oxide (Rh_2O_3) nanoparticles, International Journal of Pharmacology, *Phytochemistry and Ethnomedicine*, **1(1)**, 15–19.

3. Heidari, A. (2016) An experimental biospectroscopic study on seminal plasma in determination of semen quality for evaluation of male infertility, *Int. J. Adv. Technol.*, **7**, 007.

4. Heidari, A. (2016) Extraction and preconcentration of n–tolyl–sulfonyl–phosphoramid–saeure–dichlorid as an anti–cancer drug from plants: A pharmacognosy study, *J. Pharmacogn. Nat. Prod.*, **2**, 103.

5. Heidari, A. (2016) A thermodynamic study on hydration and dehydration of DNA and RNA−amphiphile complexes, *J. Bioeng. Biomed. Sci.*, **006**.

6. Heidari, A. (2016) Computational studies on molecular structures and carbonyl and ketene groups' effects of singlet and triplet energies of azidoketene O=C=CH–NNN and isocyanatoketene O=C=CH–N=C=O, *J. Appl. Computat. Math.* **5**, 142.

7. Heidari, A. (2016) Study of irradiations to enhance the induces the dissociation of hydrogen bonds between peptide chains and transition from helix structure to random coil structure using ATR–FTIR, Raman and ^{1}HNMR spectroscopies, *J. Biomol. Res. Ther.*, **5**, 146.

8. Heidari, A. (2016) Future prospects of point fluorescence spectroscopy, fluorescence imaging and fluorescence endoscopy in photodynamic therapy (PDT) for cancer cells, *J. Bioanal. Biomed.*, **8**, 135.

9. Heidari, A. (2016) A bio–spectroscopic study of DNA density and color role as determining factor for absorbed irradiation in cancer cells, *Adv. Cancer Prev.*, **1**, 102.

10. Heidari, A. (2016) Manufacturing process of solar cells using cadmium oxide (CdO) and rhodium (III) oxide (Rh_2O_3) nanoparticles, *J. Biotechnol. Biomater.*, **6**, 125.

11. Heidari, A. (2016) A novel experimental and computational approach to photobiosimulation of telomeric DNA/RNA: A biospectroscopic and photobiological study, *J. Res. Development*, **4**, 144.

12. Heidari, A. (2016) Biochemical and pharmacodynamical study of microporous molecularly imprinted polymer selective for vancomycin, teicoplanin, oritavancin, telavancin and dalbavancin binding, *Biochem. Physiol.*, **5**, 146.

13. Heidari, A. (2016) Anti–cancer effect of UV irradiation at presence of cadmium oxide (CdO) nanoparticles on DNA of cancer cells: A photodynamic therapy study, *Arch Cancer Res*., **4**, 1.

14. Heidari, A. (2016) Biospectroscopic study on multi–component reactions (MCRs) in two a–type and b–type conformations of nucleic acids to determine ligand binding modes, binding constant and stability of nucleic acids in cadmium oxide (CdO) nanoparticles–nucleic acids complexes as anti–cancer drugs, *Arch Cancer Res*., **4**, 2.

15. Heidari, A. (2016) Simulation of temperature distribution of DNA/RNA of human cancer cells using time–dependent bio–heat equation and Nd: YAG lasers, *Arch Cancer Res*., **4**, 2.

16. Heidari, A. (2016) Quantitative structure–activity relationship (QSAR) approximation for cadmium

oxide (CdO) and rhodium (III) oxide (Rh_2O_3) nanoparticles as anti–cancer drugs for the catalytic formation of proviral DNA from viral RNA using multiple linear and non–linear correlation approach, *Ann. Clin. Lab. Res*., **4**, 1.

17. Heidari, A. (2016) Biomedical study of cancer cells DNA therapy using laser irradiations at presence of intelligent nanoparticles, *J. Biomedical Sci*., **5**, 2.

18. Heidari, A. (2016) Measurement the amount of vitamin D2 (ergocalciferol), vitamin D3 (cholecalciferol) and absorbable calcium (Ca^{2+}), iron (II) (Fe^{2+}), magnesium (Mg^{2+}), phosphate (PO^{4-}) and zinc (Zn^{2+}) in apricot using high–performance liquid chromatography (HPLC) and spectroscopic techniques, *J. Biom. Biostat.*, **7**, 292.

19. Heidari, A. (2016) Spectroscopy and quantum mechanics of the helium dimer (He^{2+}), neon dimer (Ne^{2+}), argon dimer (Ar^{2+}), krypton dimer (Kr^{2+}), xenon dimer (Xe^{2+}), radon dimer(Rn^{2+}) and ununoctium dimer (Uuo^{2+}) molecular cations, *Chem. Sci. J.*, **7**, 112.

20. Heidari, A. (2016) Human toxicity photodynamic therapy studies on DNA/RNA complexes as a promising new sensitizer for the treatment of malignant tumors using bio–spectroscopic techniques, *J. Drug Metab. Toxicol.*, **7**, 129.

21. Heidari, A. (2016) Novel and stable modifications of intelligent cadmium oxide (CdO) nanoparticles as anti–cancer drug in formation of nucleic acids complexes for human cancer cells' treatment, *Biochem. Pharmacol.* (Los Angel), **5**, 207.

22. Heidari, A. (2016) A Combined computational and QM/MM molecular dynamics study on boron nitride nanotubes (BNNTs), amorphous boron nitride nanotubes (a–BNNTs) and hexagonal boron nitride nanotubes (h–BNNTs) as hydrogen storage, *Struct. Chem. Crystallogr. Commun.*, **2**, 1.

23. Heidari, A. (2016) Pharmaceutical and analytical chemistry study of cadmium oxide (CdO) nanoparticles synthesis methods and properties as anti–cancer drug and its effect on human cancer cells, *Pharm. Anal. Chem. Open Access*, **2**, 113.

24. Heidari, A. (2016) A chemotherapeutic and biospectroscopic investigation of the interaction of double–standard DNA/RNA–binding molecules with cadmium oxide (CdO) and rhodium (III) oxide (Rh_2O_3) nanoparticles as anti–cancer drugs for cancer cells' treatment, *Chemo. Open Access*, **5**, 129.

25. Heidari, A. (2016) Pharmacokinetics and experimental therapeutic study of DNA and other biomolecules using lasers: Advantages and applications, *J. Pharmacokinet Exp. Ther.*, **1**, 005.

26. Heidari, A. (2016) Determination of ratio and stability constant of DNA/RNA in human cancer cells and cadmium oxide (CdO) nanoparticles complexes using analytical electrochemical and spectroscopic techniques, *Insights Anal. Electrochem.*, **2**, 1.

27. Heidari, A. (2016) Discriminate between antibacterial and non–antibacterial drugs artificial neutral networks of a multilayer perceptron (MLP) type using a set of topological descriptors, *J. Heavy Met. Toxicity Dis*., **1**, 2.

28. Heidari, A. (2016) Combined theoretical and computational study of the belousov–zhabotinsky chaotic reaction and curtius rearrangement for synthesis of mechlorethamine, cisplatin, streptozotocin, cyclophosphamide, melphalan, busulphan and BCNU as anti–cancer drugs, *Insights Med. Phys*., **1**, 2.

29. Heidari, A. (2016) A translational biomedical approach to structural arrangement of amino acids' complexes: A combined theoretical and computational study, *Transl. Biomed*., **7**, 2.

30. Heidari, A. (2016) Ab initio and density functional theory (DFT) studies of dynamic NMR shielding tensors and vibrational frequencies of DNA/RNA and cadmium oxide (CdO) nanoparticles complexes in human cancer cells, *J. Nanomedine Biotherapeutic Discov.*, **6**, 144.

31. Heidari, A. (2016) Molecular dynamics and monte–carlo simulations for replacement sugars in insulin resistance, obesity, LDL cholesterol, triglycerides, metabolic syndrome, type 2 diabetes and cardiovascular disease: A glycobiological study, *J. Glycobiol.*, **5**, 111.

32. Heidari, A. (2016) Synthesis and study of 5–[(phenylsulfonyl)amino]–1,3,4–thiadiazole–2–sulfonamide as potential anti–pertussis drug using chromatography and spectroscopy techniques, *Transl. Med.* (Sunnyvale), **6**, 138.

33. Heidari, A. (2016) Nitrogen, oxygen, phosphorus and sulphur heterocyclic anti–cancer nano drugs separation in the supercritical fluid of ozone (O_3) using soave–redlich–kwong (SRK) and pang–robinson (PR) equations, *Electronic J. Biol.*, **12**, 4.

34. Heidari, A. (2016) An analytical and computational

infrared spectroscopic Review of vibrational modes in nucleic acids, *Austin J. Anal. Pharm. Chem*., **3(1)**, 1058.

35. Heidari, A., Brown, C. (2016) Phase, composition and morphology study and analysis of Os–Pd/HfC nanocomposites, *Nano Res. Appl*., **2**, 1.

36. Heidari, A., Brown, C. (2016) Vibrational spectroscopic study of intensities and shifts of symmetric vibration modes of ozone diluted by cumene, *International Journal of Advanced Chemistry*, **4(1)**, 5–9.

37. Heidari, A. (2016) Study of the role of anti–cancer molecules with different sizes for decreasing corresponding bulk tumor multiple organs or tissues, *Arch Can Res*., **4**, 2.

38. Heidari, A. (2016) Genomics and proteomics studies of zolpidem, necopidem, alpidem, saripidem, miroprofen, zolimidine, olprinone and abafungin as anti–tumor, peptide antibiotics, antiviral and central nervous system (CNS) drugs, *J. Data Mining Genomics & Proteomics*, **7**, 125.

39. Heidari, A. (2016) Pharmacogenomics and pharmacoproteomics studies of phosphor-diesterase–5 (PDE5) inhibitors and paclitaxel albumin–stabilized nanoparticles as sandwiched anti–cancer nano drugs between two DNA/RNA molecules of human cancer cells, *J. Pharmacogenomics Pharmacoproteomics*, **7**, 153.

40. Heidari, A. (2016) Biotranslational medical and biospectroscopic studies of cadmium oxide (CdO) nanoparticles–DNA/RNA straight and cycle chain complexes as potent anti–viral, anti–tumor and anti–microbial drugs: A clinical approach, *Transl. Biomed*., **7**, 2.

41. Heidari, A. (2016) A Comparative study on simultaneous determination and separation of adsorbed cadmium oxide (CdO) nanoparticles on DNA/RNA of human cancer cells using biospectroscopic techniques and dielectrophoresis (DEP) method, *Arch Can Res*., **4**, 2.

42. Heidari, A. (2016) Cheminformatics and system chemistry of cisplatin, carboplatin, nedaplatin, oxaliplatin, heptaplatin and lobaplatin as anti–cancer nano drugs: A combined computational and experimental study, *J. Inform Data Min.*, **1**, 3.

43. Heidari, A. (2016) Linear and non–linear quantitative structure–anti–cancer–activity relationship (QSACAR) study of hydrous ruthenium (IV) oxide (RuO_2) nanoparticles as non–nucleoside reverse transcriptase inhibitors (NNRTIs) and anti–cancer nano drugs, *J. Integr. Oncol.*, **5**, 110.

44. Heidari, A. (2016) Synthesis, characterization and biospectroscopic studies of cadmium oxide (CdO) nanoparticles–nucleic acids complexes absence of soluble polymer as a protective agent using nucleic acids condensation and solution reduction method, *J. Nanosci. Curr. Res.*, **1**, 101.

45. Heidari, A. (2016) Coplanarity and collinearity of 4'–dinonyl–2,2'–bithiazole in one domain of bleomycin and pingyangmycin to be responsible for binding of cadmium oxide (CdO) nanoparticles to DNA/RNA bidentate ligands as anti–tumor nano drug, *Int. J. Drug Dev. & Res.*, **8**, 7–8.

46. Heidari, A. (2016) A pharmacovigilance study on linear and non–linear quantitative structure (chromatographic) retention relationships (QSRR) models for the prediction of retention time of anti–cancer nano drugs under synchrotron radiations, *J. Pharmacovigil*, **4**, 161.

47. Heidari, A. (2016) Nanotechnology in preparation of semipermeable polymers, *J. Adv. Chem. Eng.*, **6**, 157.

48. Heidari, A. (2016) A gastrointestinal study on linear and non–linear quantitative structure (chromatographic) retention relationships (QSRR) models for analysis 5–aminosalicylates nano particles as digestive system nano drugs under synchrotron radiations, *J. Gastrointest Dig Syst.*, **6**, 119.

49. Heidari, A. (2016) DNA/RNA fragmentation and cytolysis in human cancer cells treated with diphthamide nano particles derivatives, *Biomedical Data Mining*, **5**, 102.

50. Heidari, A. (2016) A successful strategy for the prediction of solubility in the construction of quantitative structure–activity relationship (QSAR) and quantitative structure–property relationship (QSPR) under synchrotron radiations using genetic function approximation (GFA) algorithm, *J. Mol. Biol. Biotechnol.*, **1**, 1.

51. Heidari, A. (2016) Computational study on molecular structures of C_{20}, C_{60}, C_{240}, C_{540}, C_{960}, C_{2160} and C_{3840} fullerene nano molecules under synchrotron radiations using fuzzy logic, *J. Material Sci. Eng.*, **5**, 282.

52. Heidari, A. (2016) Graph theoretical analysis of zigzag polyhexamethylene biguanide, polyhexa-

methylene adipamide, polyhexamethylene biguanide gauze and polyhexamethylene biguanide hydrochloride (PHMB) boron nitride nanotubes (BNNTs), amorphous boron nitride nanotubes (a–BNNTs) and hexagonal boron nitride nanotubes (h–BNNTs), *J. Appl. Computat. Math.*, **5**, 143.

53. Heidari, A. (2016) The impact of high resolution imaging on diagnosis, *Int. J. Clin. Med. Imaging*, **3**, 1000e101.

54. Heidari, A. (2016) A comparative study of conformational behavior of isotretinoin (13–cis retinoic acid) and tretinoin (all–trans retinoic acid (ATRA)) nano particles as anti–cancer nano drugs under synchrotron radiations using Hartree–Fock (HF) and density functional theory (DFT) methods, *Insights in Biomed.*, **1**, 2.

55. Heidari, A. (2016) Advances in logic, operations and computational mathematics, *J. Appl. Computat. Math.*, **5**, 5.

56. Heidari, A. (2016) Mathematical equations in predicting physical behavior, *J. Appl. Computat. Math.*, **5**, 5.

57. Heidari, A. (2016) Chemotherapy a last resort for cancer treatment, *Chemo Open Access*, **5**, 4.

58. Heidari, A. (2016) Separation and pre–concentration of metal cations–DNA/RNA chelates using molecular beam mass spectrometry with tunable vacuum ultraviolet (VUV) synchrotron radiation and various analytical methods, *Mass Spectrom Purif Tech.*, **2**, 101.

59. Heidari, (2016) A. Yoctosecond quantitative structure–activity relationship (QSAR) and quantitative structure–property relationship (QSPR) under synchrotron radiations studies for prediction of solubility of anti–cancer nano drugs in aqueous solutions using genetic function approximation (GFA) algorithm, *Insight Pharm. Res.*, **1**, 1.

60. Heidari, A. (2016) Cancer risk prediction and assessment in human cells under synchrotron radiations using quantitative structure activity relationship (QSAR) and quantitative structure properties relationship (QSPR) studies, *Int. J. Clin. Med. Imaging*, **3**, 516.

61. Heidari, A. (2016) A novel approach to biology, *Electronic J. Biol.* **12**, 4.

62. Heidari, A. (2016) Innovative biomedical equipment's for diagnosis and treatment, *J. Bio-engineer & Biomedical Sci.*, **6**, 2.

63. Heidari, A. (2016) Integrating precision cancer medicine into healthcare, medicare reimbursement changes and the practice of oncology: Trends in oncology medicine and practices, *J. Oncol Med. & Pract.*, **1**, 2.

64. Heidari, A. (2016) Promoting convergence in biomedical and biomaterials sciences and silk proteins for biomedical and biomaterials applications: An introduction to materials in medicine and bioengineering perspectives, *J. Bioengineer & Biomedical Sci.*, **6**, 3.

65. Heidari, A. (2017) X–ray fluorescence and x–ray diffraction analysis on discrete element modeling of nano powder metallurgy processes in optimal container design, *J. Powder Metall. Min.*, **6**, 1.

66. Heidari, A. (2017) Biomolecular spectroscopy and dynamics of nano–sized molecules and clusters as cross–linking–induced anti–cancer and immune–oncology nano drugs delivery in DNA/RNA of human cancer cells' membranes under synchrotron radiations: A payload–based perspective, *Arch Chem. Res.*, **1**, 2.

67. Heidari, A. (2017) Deficiencies in repair of double–standard DNA/RNA–binding molecules identified in many types of solid and liquid tumors oncology in human body for advancing cancer immunotherapy using computer simulations and data analysis: Number of mutations in a synchronous tumor varies by age and type of synchronous cancer, *J. Appl. Bioinforma. Comput. Biol.*, **6**, 1.

68. Heidari, A. (2017) Electronic coupling among the five nanomolecules shuts down quantum tunneling in the presence and absence of an applied magnetic field for indication of the dimer or other provide different influences on the magnetic behavior of single molecular magnets (SMMs) as qubits for quantum computing, *Glob. J. Res. Rev.*, **4**, 2.

69. Heidari, A. (2017) Polymorphism in nano–sized graphene ligand–induced transformation of Au_{38}–$xAg_x/xCu_x(SPh–tBu)_{24}$ to Au_{36}–$xAg_x/xCu_x(SPh–tBu)_{24}$ (x = 1–12) nanomolecules for synthesis of Au_{144}–$xAg_x/xCu_x[(SR)_{60}$, $(SC_4)_{60}$, $(SC_6)_{60}$, $(SC_{12})_{60}$, $(PET)_{60}$, $(p–MBA)_{60}$, $(F)_{60}$, $(Cl)_{60}$, $(Br)_{60}$, $(I)_{60}$, $(At)_{60}$, $(Uus)_{60}$ and $(SC_6H_{13})_{60}]$ nano clusters as anti–cancer nano drugs, *J. Nanomater. Mol Nanotechnol.*, **6**, 3.

70. Heidari, A. (2017) Biomedical resource oncology and data mining to enable resource discovery in

medical, medicinal, clinical, pharmaceutical, chemical and translational research and their applications in cancer research, *Int. J. Biomed. Data Min.,* **6**, 103.

71. Heidari, A. (2017) Study of synthesis, pharmacokinetics, pharmacodynamics, dosing, stability, safety and efficacy of olympiadane nanomolecules as agent for Cancer Enzymo-therapy, Immunotherapy, Chemotherapy, Radio-therapy, hormone therapy and targeted therapy under synchrotorn radiation, *J. Dev. Drugs* **6**, 154.

72. Heidari, A. (2017) A novel approach to future horizon of top seven biomedical research topics to watch in 2017: Alzheimer's, ebola, hypersomnia, human immunodeficiency virus (HIV), tuber-culosis (TB), microbiome/antibiotic resistance and endovascular stroke, *J. Bioengineer & Biomedical Sci.,* **7**, 127.

73. Heidari, A. (2017) Opinion on computational fluid dynamics (CFD) technique, *Fluid Mech Open Acc.,* **4**, 157.

74. Heidari, A. (2017) Concurrent diagnosis of oncology influence outcomes in emergency general surgery for colorectal cancer and multiple sclerosis (MS) treatment using magnetic resonance imaging (MRI) and $Au_{329}(SR)_{84}$, $Au_{329-x}Ag_x(SR)_{84}$, $Au_{144}(SR)_{60}$, $Au_{68}(SR)_{36}$, $Au_{30}(SR)_{18}$, $Au_{102}(SPh)_{44}$, $Au_{38}(SPh)_{24}$, $Au_{38}(SC_2H_4Ph)_{24}$, $Au_{21}S(SAdm)_{15}$, $Au_{36}(pMBA)_{24}$ and $Au_{25}(pMBA)_{18}$ nano clusters, *J. Surgery Emerg. Med.,* **1**, 21.

75. Heidari, A. (2017) Developmental cell biology in adult stem cells death and autophagy to trigger a preventive allergic reaction to common airborne allergens under synchrotron radiation using nanotechnology for therapeutic goals in particular allergy shots (immunotherapy), *Cell Biol.* (Henderson, NV), **6**, 1.

76. Heidari, A. (2017) Changing metal powder characteristics for elimination of the heavy metals toxicity and diseases in disruption of extracellular matrix (ECM) proteins adjustment in cancer metastases induced by osteosarcoma, chondrosarcoma, carcinoid, carcinoma, ewing's sarcoma, fibrosarcoma and secondary hematopoietic solid or soft tissue tumors, *J. Powder Metall. Min.,* **6**, 170.

77. Heidari, A. (2017) Nanomedicine–based combination anti–cancer therapy between nucleic acids and anti–cancer nano drugs in covalent nano drugs delivery systems for selective imaging and treatment of human brain tumors using hyaluronic acid, alguronic acid and sodium hyaluronate as anti–cancer nano drugs and nucleic acids delivery under synchrotron radiation, *Am. J. Drug Deliv.,* **5**, 2.

78. Heidari, A. (2017) Clinical trials of dendritic cell therapies for cancer exposing vulnerabilities in human cancer cells' metabolism and metabolomics: New discoveries, unique features inform new therapeutic opportunities, biotech's bumpy road to the market and elucidating the biochemical programs that support cancer initiation and progression, *J. Biol. Med. Science,* **1**, 103.

79. Heidari, A. (2017) The design graphene–based nanosheets as a new nanomaterial in anti–cancer therapy and delivery of chemotherapeutics and biological nano drugs for liposomal anti–cancer nano drugs and gene delivery, *Br. Biomed. Bull,* **5**: 305.

80. Heidari, A. (2017) Integrative approach to biological networks for emerging roles of proteomics, genomics and transcriptomics in the discovery and validation of human colorectal cancer biomarkers from DNA/RNA sequencing data under synchrotron radiation, *Transcriptomics,* **5**, 117.

81. Heidari, A. (2017) Elimination of the heavy metals toxicity and diseases in disruption of extracellular matrix (ECM) proteins and cell adhesion intelligent nanomolecules adjustment in cancer metastases using metalloenzymes and under synchrotron radiation, *Lett Health Biol. Sci.,* **2(2)**, 1–4.

82. Heidari, A. (2017) Treatment of breast cancer brain metastases through a targeted nanomolecule drug delivery system based on dopamine functionalized multi–wall carbon nanotubes (MWCNTs) coated with nano graphene oxide (GO) and protonated polyaniline (PANI) in situ during the polymerization of aniline autogenic nanoparticles for the delivery of anti–cancer nano drugs under synchrotron radiation, *Br J. Res.,* **4(3)**, 16.

83. Heidari, A. Sedative, (2017) Analgesic and ultrasound–mediated gastrointestinal nano drugs delivery for gastrointestinal endoscopic procedure, nano drug–induced gastrointestinal disorders and nano drug treatment of gastric acidity, *Res. Rep. Gastroenterol,* **1**, 1.

84. Heidari, A. (2017) Synthesis, pharmacokinetics, pharmacodynamics, dosing, stability, safety and efficacy of orphan nano drugs to treat high cholesterol and related conditions and to prevent cardiovascular disease under synchrotron

radiation, *J. Pharm. Sci. Emerg. Drugs*, **5**, 1.

85. Heidari, A. (2017) Non–linear compact proton synchrotrons to improve human cancer cells and tissues treatments and diagnostics through particle therapy accelerators with monochromatic microbeams, *J. Cell Biol. Mol Sci.,* **2(1)**, 1–5.

86. Heidari, A. (2017) Design of targeted metal chelation therapeutics nanocapsules as colloidal carriers and blood–brain barrier (BBB) translocation to targeted deliver anti–cancer nano drugs into the human brain to treat alzheimer's disease under synchrotron radiation, *J. Nanotechnol. Material Sci.,* **4(2)**, 1–5.

87. Gobato, R., Haidari, A. (2017) Calculations using quantum chemistry for inorganic molecule simulation $BeLi_2SeSi$, *Science Journal of Analytical Chemistry*, **5(6)**, 76–85.

88. Heidari, A. (2017) Different high–resolution simulations of medical, medicinal, clinical, pharmaceutical and therapeutics oncology of human lung cancer translational anti–cancer nano drugs delivery treatment process under synchrotron and x–ray radiations, *J. Med. Oncol*., **1(1)**, 1.

89. Heidari, A. (2017) A modern ethno-medicinal technique for transformation, prevention and treatment of human malignant gliomas tumors into human benign gliomas tumors under synchrotron radiation, *Am. J. Ethnomed.*, **4(1)**, 10.

90. Heidari, A. (2017) Active targeted nanoparticles for anti–cancer nano drugs delivery across the blood–brain barrier for human brain cancer treatment, multiple sclerosis (MS) and alzheimer's diseases using chemical modifications of anti–cancer nano drugs or drug–nanoparticles through zika virus (ZIKV) nanocarriers under synchrotron radiation, *J. Med. Chem. Toxicol.*, **2(3)**, 1–5.

91. Heidari, A. (2017) Investigation of medical, medicinal, clinical and pharmaceutical applications of estradiol, mestranol (norlutin), norethindrone (NET), norethisterone acetate (NETA), norethisterone enanthate (NETE) and testosterone nanoparticles as biological imaging, cell labeling, anti–microbial agents and anti–cancer nano drugs in nanomedicines based drug delivery systems for anti–cancer targeting and treatment, *Parana Journal of Science and Education (PJSE)*, **3(4)**, 10–19.

92. Heidari, A. (2017) A comparative computational and experimental study on different vibrational biospectroscopy methods, techniques and applications for human cancer cells in tumor tissues simulation, modeling, research, diagnosis and treatment, *Open J. Anal Bioanal. Chem.,* **1(1)**, 14–20.

93. Heidari, A. (2017) Combination of DNA/RNA ligands and linear/non–linear visible–synchrotron radiation–driven n–doped ordered mesoporous cadmium oxide (CdO) nanoparticles photocatalysts channels resulted in an interesting synergistic effect enhancing catalytic anti–cancer activity, *Enz. Eng.,* **6**, 1.

94. Heidari, A. (2017) Modern approaches in designing ferritin, ferritin light chain, transferrin, beta–2 transferrin and bacterioferritin–based anti–cancer nano drugs encapsulating nanosphere as DNA–binding proteins from starved cells (DPS), *Mod Appro. Drug Des*., **1(1)**, MADD.000504.

95. Heidari, A. (2017) Potency of human interferon β–1a and human interferon β–1b in enzymotherapy, immunotherapy, chemotherapy, radiotherapy, hormone therapy and targeted therapy of encephalomyelitis disseminate/multiple sclerosis (MS) and hepatitis A, B, C, D, E, F and G virus enter and targets liver cells, *J. Proteomics Enzymol,* **6**, 1.

96. Heidari, A. (2017) Transport therapeutic active targeting of human brain tumors enable anti–cancer nanodrugs delivery across the blood–brain barrier (BBB) to treat brain diseases using nanoparticles and nanocarriers under synchrotron radiation, *J. Pharm. Pharmaceutics*, **4(2)**, 1–5.

97. Heidari, A., Brown C. (2017) Combinatorial therapeutic approaches to DNA/RNA and benzylpenicillin (penicillin G), fluoxetine hydrochloride (prozac and sarafem), propofol (diprivan), acetylsalicylic acid (ASA) (aspirin), naproxen sodium (aleve and naprosyn) and dextromethamphetamine nanocapsules with surface conjugated DNA/RNA to targeted nano drugs for enhanced anti–cancer efficacy and targeted cancer therapy using nano drugs delivery systems, *Ann. Adv. Chem*., **1(2)**, 61–69.

98. Heidari, A. (2017) High–resolution simulations of human brain cancer translational nano drugs delivery treatment process under synchrotron radiation, *J. Transl. Res*., **1(1)**, 1–3.

99. Heidari, A. (2017) Investigation of anti–cancer nano drugs' effects' trend on human pancreas cancer cells and tissues prevention, diagnosis and treatment process under synchrotron and x–ray

radiations with the passage of time using mathematica, *Current Trends Anal Bioanal Chem.*, **1(1)**, 36–41.

100. Heidari, A. (2017) Pros and cons controversy on molecular imaging and dynamics of double–standard DNA/RNA of human preserving stem cells–binding nano molecules with androgens/anabolic steroids (AAS) or testosterone derivatives through tracking of helium–4 nucleus (alpha particle) using synchrotron radiation, *Arch Biotechnol. Biomed*., **1(1)**, 067–0100.

101. Heidari, A. (2017) Visualizing metabolic changes in probing human cancer cells and tissues metabolism using vivo ^{1}H or proton NMR, ^{13}C NMR, ^{15}N NMR and ^{31}P NMR spectroscopy and self–organizing maps under synchrotron radiation, *SOJ Mater. Sci. Eng.*, **5(2)**, 1–6.

102. Heidari, A. (2017) Cavity ring–down spectroscopy (CRDS), circular dichroism spectroscopy, cold vapour atomic fluorescence spectroscopy and correlation spectroscopy comparative study on malignant and benign human cancer cells and tissues with the passage of time under synchrotron radiation, *Enliven: Challenges Cancer Detect Ther.*, **4(2)**, 001.

103. Heidari, A. (2017) laser spectroscopy, laser–induced breakdown spectroscopy and laser–induced plasma spectroscopy comparative study on malignant and benign human cancer cells and tissues with the passage of time under synchrotron radiation, *Int. J. Hepatol Gastroenterol*, **3(4)**, 79–84.

104. Heidari, A. (2017) Time–resolved spectroscopy and time–stretch spectroscopy comparative study on malignant and benign human cancer cells and tissues with the passage of time under synchrotron radiation, *Enliven: Pharmacovigilance and Drug Safety*, **4(2)**, 001.

105. Heidari, A. (2017) Overview of the role of vitamins in reducing negative effect of decapeptyl (triptorelin acetate or pamoate salts) on prostate cancer cells and tissues in prostate cancer treatment process through transformation of malignant prostate tumors into benign prostate tumors under synchrotron radiation, *Open J. Anal Bioanal Chem.*, **1(1)**, 21–26.

106. Heidari, A. (2017) Electron phenomenological spectroscopy, electron paramagnetic resonance (EPR) spectroscopy and electron spin resonance (ESR) spectroscopy comparative study on malignant and benign human cancer cells and tissues with the passage of time under synchrotron radiation, *Austin J. Anal Pharm. Chem*., **4(3)**, 1091.

107. Heidari, A. (2017) Therapeutic nanomedicine different high–resolution experimental images and computational simulations for human brain cancer cells and tissues using nanocarriers deliver DNA/RNA to brain tumors under synchrotron radiation with the passage of time using mathematica and MATLAB, *Madridge J. Nano Tech. Sci.*, **2(2)**, 77–83.

108. Heidari, A. (2017) A consensus and prospective study on restoring cadmium oxide (CdO) nanoparticles sensitivity in recurrent ovarian cancer by extending the cadmium oxide (CdO) nanoparticles–free interval using synchrotron radiation therapy as antibody–drug conjugate for the treatment of limited–stage small cell diverse epithelial cancers, *Cancer Clin. Res. Rep.*, **1(2)**, 001.

109. Heidari, A. (2017) A novel and modern experimental imaging and spectroscopy comparative study on malignant and benign human cancer cells and tissues with the passage of time under white synchrotron radiation, *Cancer Sci. Res. Open Access*, **4(2)**, 1–8.

110. Heidari, A. (2017) Different high–resolution simulations of medical, medicinal, clinical, pharmaceutical and therapeutics oncology of human breast cancer translational nano drugs delivery treatment process under synchrotron and x–ray radiations, *J. Oral Cancer Res.*, **1(1)**, 12–17.

111. Heidari, A. (2017) Vibrational decihertz (dHz), centihertz (cHz), millihertz (mHz), microhertz (μHz), nanohertz (nHz), picohertz (pHz), femtohertz (fHz), attohertz (aHz), zeptohertz (zHz) and yoctohertz (yHz) imaging and spectroscopy comparative study on malignant and benign human cancer cells and tissues under synchrotron radiation, *International Journal of Biomedicine*, **7(4)**, 335–340.

112. Heidari, A. (2017) Force spectroscopy and fluorescence spectroscopy comparative study on malignant and benign human cancer cells and tissues with the passage of time under synchrotron radiation, *EC Cancer*, **2(5)**, 239–246.

113. Heidari, A. (2017) Photoacoustic spectroscopy, photoemission spectroscopy and photothermal spectroscopy comparative study on malignant and benign human cancer cells and tissues with the passage of time under synchrotron radiation, *BAOJ Cancer Res. Ther.*, **3(3)**, 45–52.

114. Heidari, A. (2017) J–spectroscopy, exchange spectroscopy (EXSY), nuclear overhauser effect spectroscopy (NOESY) and total correlation spectroscopy (TOCSY) comparative study on malignant and benign human cancer cells and tissues under synchrotron radiation, *EMS Eng. Sci. J.*, **1(2)**, 6–13.

115. Heidari, A. (2017) Neutron spin echo spectroscopy and spin noise spectroscopy comparative study on malignant and benign human cancer cells and tissues with the passage of time under synchrotron radiation, *Int. J. Biopharm. Sci.*, **1**, 103–107.

116. Heidari, A. (2017) Vibrational decahertz (daHz), hectohertz (hHz), kilohertz (kHz), megahertz (MHz), gigahertz (GHz), terahertz (THz), petahertz (PHz), exahertz (EHz), zettahertz (ZHz) and yottahertz (YHz) imaging and spectroscopy comparative study on malignant and benign human cancer cells and tissues under synchrotron radiation, *Madridge J. Anal Sci. Instrum.*, **2(1)**, 41–46.

117. Heidari, A. (2018) Two–dimensional infrared correlation spectroscopy, linear two–dimensional infrared spectroscopy and non–linear two–dimensional infrared spectroscopy comparative study on malignant and benign human cancer cells and tissues under synchrotron radiation with the passage of time, *J. Mater Sci. Nanotechnol.*, **6(1)**, 101.

118. Heidari, A. (2018) Fourier transform infrared (FTIR) spectroscopy, near–infrared spectroscopy (NIRS) and mid–infrared spectroscopy (MIRS) comparative study on malignant and benign human cancer cells and tissues under synchrotron radiation with the passage of time, *Int. J. Nanotechnol. Nanomed.*, **3(1)**, 1–6.

119. Heidari, A. (2018) Infrared photo dissociation spectroscopy and infrared correlation table spectroscopy comparative study on malignant and benign human cancer cells and tissues under synchrotron radiation with the passage of time, *Austin Pharmacol. Pharm.*, **3(1)**, 1011.

120. Heidari, A. (2017) Novel and transcendental prevention, diagnosis and treatment strategies for investigation of interaction among human blood cancer cells, tissues, tumors and metastases with synchrotron radiation under anti–cancer nano drugs delivery efficacy using MATLAB modeling and simulation, *Madridge J. Nov. Drug Res.*, **1(1)**, 18–24.

121. Heidari, A. (2018) Comparative study on malignant and benign human cancer cells and tissues with the passage of time under synchrotron radiation, *Open Access J. Trans. Med. Res.*, **2(1)**, 26–32.

122. Gobato, M.R.R., Gobato, R., Heidari, A. (2018) Planting of jaboticaba trees for landscape repair of degraded area, *Landscape Architecture and Regional Planning*, **3(1)**, 1–9.

123. Heidari, A. (2018) Fluorescence spectroscopy, phosphorescence spectroscopy and luminescence spectroscopy comparative study on malignant and benign human cancer cells and tissues under synchrotron radiation with the passage of time, *SM J. Clin. Med. Imaging*, **4(1)**, 1018.

124. Heidari, A. (2018) Nuclear inelastic scattering spectroscopy (NISS) and nuclear inelastic absorption spectroscopy (NIAS) comparative study on malignant and benign human cancer cells and tissues under synchrotron radiation, *Int. J. Pharm. Sci.*, **2(1)**, 1–14.

125. Heidari, A. (2018) X–ray diffraction (XRD), powder x–ray diffraction (PXRD) and energy–dispersive x–ray diffraction (EDXRD) comparative study on malignant and benign human cancer cells and tissues under synchrotron radiation, *J. Oncol Res.*, **2(1)**, 1–14.

126. Heidari, A. (2018) Correlation two–dimensional nuclear magnetic resonance (NMR) (2D–NMR) (COSY) imaging and spectroscopy comparative study on malignant and benign human cancer cells and tissues under synchrotron radiation, *EMS Can Sci.*, **1**–1–001.

127. Heidari, A. (2018) Thermal spectroscopy, photothermal spectroscopy, thermal micro-spectroscopy, photothermal microspectroscopy, thermal macrospectroscopy and photothermal macrospectroscopy comparative study on malignant and benign human cancer cells and tissues with the passage of time under synchrotron radiation, *SM J. Biometrics Biostat.*, **3(1)**, 1024.

128. Heidari, A. (2018) A modern and comprehensive experimental biospectroscopic comparative study on human common cancers' cells, tissues and tumors before and after synchrotron radiation therapy, *Open Acc. J. Oncol Med*., **1(1)**.

129. Heidari, A. (2018) Heteronuclear correlation experiments such as heteronuclear single–quantum correlation spectroscopy (HSQC), heteronuclear multiple–quantum correlation spectroscopy (HMQC) and heteronuclear multiple–bond correlation spectroscopy (HMBC) comparative study on malignant and benign human

endocrinology and thyroid cancer cells and tissues under synchrotron radiation, *J. Endocrinol Thyroid Res.*, **3(1)**, 555603.

130. Heidari, A. (2018) Nuclear resonance vibrational spectroscopy (NRVS), nuclear inelastic scattering spectroscopy (NISS), nuclear inelastic absorption spectroscopy (NIAS) and nuclear resonant inelastic x–ray scattering spectroscopy (NRIXSS) comparative study on malignant and benign human cancer cells and tissues under synchrotron radiation, *Int. J. Bioorg. Chem. Mol Biol*., **6(1e)**, 1–5.

131. Heidari, A. (2018) A novel and modern experimental approach to vibrational circular dichroism spectroscopy and video spectroscopy comparative study on malignant and benign human cancer cells and tissues with the passage of time under white and monochromatic synchrotron radiation, *Glob. J. Endocrinol Metab*., **1(3)**, GJEM. 000514–000519.

132. Heidari, A. (2018) Pros and cons controversy on heteronuclear correlation experiments such as heteronuclear single–quantum correlation spectroscopy (HSQC), heteronuclear multiple–quantum correlation spectroscopy (HMQC) and heteronuclear multiple–bond correlation spectroscopy (HMBC) comparative study on malignant and benign human cancer cells and tissues under synchrotron radiation, *EMS Pharma. J*., **1(1)**, 2–8.

133. Heidari, A. (2018) A modern comparative and comprehensive experimental biospectroscopic study on different types of infrared spectroscopy of malignant and benign human cancer cells and tissues with the passage of time under synchrotron radiation, *J. Analyt. Molecul. Tech*., **3(1)**, 8.

134. Heidari, A. (2018) Investigation of cancer types using synchrotron technology for proton beam therapy: An experimental biospectroscopic comparative study, *European Modern Studies Journal*, **2(1)**, 13–29.

135. Heidari, A. (2018) Saturated spectroscopy and unsaturated spectroscopy comparative study on malignant and benign human cancer cells and tissues with the passage of time under synchrotron radiation, *Imaging J. Clin. Medical Sci*., **5(1)**, 1–7.

136. Heidari, A. (2018) Small–angle neutron scattering (SANS) and wide–angle x–ray diffraction (WAXD) comparative study on malignant and benign human cancer cells and tissues under synchrotron radiation, *Int. J. Bioorg. Chem. Mol. Biol*., **6(2e)**, 1–6.

137. Heidari, A. (2018) Investigation of bladder cancer, breast cancer, colorectal cancer, endometrial cancer, kidney cancer, leukemia, liver, lung cancer, melanoma, non–Hodgkin lymphoma, pancreatic cancer, prostate cancer, thyroid cancer and non–melanoma skin cancer using synchrotron technology for proton beam therapy: An experimental biospectroscopic comparative study, *Ther. Res. Skin Dis.*, **1(1)**.

138. Heidari, A. (2018) Attenuated total reflectance Fourier transform infrared (ATR–FTIR) spectroscopy, micro–attenuated total reflectance Fourier transform infrared (Micro–ATR–FTIR) spectroscopy and macro–attenuated total reflectance Fourier transform infrared (Macro–ATR–FTIR) spectroscopy comparative study on malignant and benign human cancer cells and tissues under synchrotron radiation with the passage of time, *International Journal of Chemistry Papers*, **2(1)**, 1–12.

139. Heidari, A. (2018) Mössbauer spectroscopy, Mössbauer emission spectroscopy and ^{57}Fe Mössbauer spectroscopy comparative study on malignant and benign human cancer cells and tissues under synchrotron radiation, *Acta Scientific Cancer Biology* **2(3)**, 17–20.

140. Heidari, A. (2018) Comparative study on malignant and benign human cancer cells and tissues under synchrotron radiation with the passage of time, *Organic & Medicinal Chem. IJ*. **6(1)**, 555676.

141. Heidari, A. (2018) Correlation spectroscopy, exclusive correlation spectroscopy and total correlation spectroscopy comparative study on malignant and benign human AIDS–related cancers cells and tissues with the passage of time under synchrotron radiation, *Int. J. Bioanal. Biomed*., **2(1)**, 1–7.

142. Heidari, A. (2018) Biomedical instrumentation and applications of biospectroscopic methods and techniques in malignant and benign human cancer cells and tissues studies under synchrotron radiation and anti–cancer nano drugs delivery, *Am. J. Nanotechnol. Nanomed*., **1(1)**, 1–9.

143. Heidari, A. (2018) Vivo ^{1}H or proton NMR, ^{13}C NMR, ^{15}N NMR and ^{31}P NMR spectroscopy comparative study on malignant and benign human cancer cells and tissues under synchrotron radiation, *Ann. Biomet. Biostat*., **1(1)**, 1001.

144. Heidari, A. (2018) Grazing–incidence small–angle neutron scattering (GISANS) and grazing–

incidence x–ray diffraction (GIXD) comparative study on malignant and benign human cancer cells, tissues and tumors under synchrotron radiation, *Ann. Cardiovasc. Surg*., **1(2)**, 1006.

145. Heidari, A. (2018) Adsorption isotherms and kinetics of multi–walled carbon nanotubes (MWCNTs), boron nitride nanotubes (BNNTs), amorphous boron nitride nanotubes (a–BNNTs) and hexagonal boron nitride nanotubes (h–BNNTs) for eliminating carcinoma, sarcoma, lymphoma, leukemia, germ cell tumor and blastoma cancer cells and tissues, *Clin. Med. Rev. Case Rep.,* **5**, 201.

146. Heidari, A. (2018) Correlation spectroscopy (COSY), exclusive correlation spectroscopy (ECOSY), total correlation spectroscopy (TOCSY), incredible natural–abundance double–quantum transfer experiment (INADEQUATE), heteronuclear single–quantum correlation spectroscopy (HSQC), heteronuclear multiple–bond correlation spectroscopy (HMBC), nuclear Overhauser effect spectroscopy (NOESY) and rotating frame nuclear Overhauser effect spectroscopy (ROESY) comparative study on malignant and benign human cancer cells and tissues under synchrotron radiation, *Acta Scientific Pharmaceutical Sciences,* **2(5)**, 30–35.

147. Heidari, A. (2018) Small–angle x–ray scattering (SAXS), ultra–small angle x–ray scattering (USAXS), fluctuation x–ray scattering (FXS), wide–angle x–ray scattering (WAXS), grazing–incidence small–angle x–ray scattering (GISAXS), grazing–incidence wide–angle x–ray scattering (GIWAXS), small–angle neutron scattering (SANS), grazing–incidence small–angle neutron scattering (GISANS), x–ray diffraction (XRD), powder x–ray diffraction (PXRD), wide–angle x–ray diffraction (WAXD), grazing–incidence x–ray diffraction (GIXD) and energy–dispersive x–ray diffraction (EDXRD) comparative study on malignant and benign human cancer cells and tissues under synchrotron radiation, *Oncol Res. Rev.*, **1(1)**, 1–10.

148. Heidari, A. (2018) Pump–probe spectroscopy and transient grating spectroscopy comparative study on malignant and benign human cancer cells and tissues with the passage of time under synchrotron radiation, *Adv. Material Sci. Engg.*, **2(1)**, 1–7.

149. Heidari, A. (2018) Grazing–incidence small–angle x–ray scattering (GISAXS) and grazing–incidence wide–angle x–ray scattering (GIWAXS) comparative study on malignant and benign human cancer cells and tissues under synchrotron radiation, *Insights Pharmacol. Pharm. Sci.,* **1(1)**, 1–8.

150. Heidari, A. (2018) Acoustic spectroscopy, acoustic resonance spectroscopy and auger spectroscopy comparative study on anti–cancer nano drugs delivery in malignant and benign human cancer cells and tissues with the passage of time under synchrotron radiation, *Nanosci. Technol.,* **5(1)**, 1–9.

151. Heidari, A. (2018) Niobium, technetium, ruthenium, rhodium, hafnium, rhenium, osmium and iridium ions incorporation into the nano polymeric matrix (NPM) by immersion of the nano polymeric modified electrode (NPME) as molecular enzymes and drug targets for human cancer cells, tissues and tumors treatment under synchrotron and synchrocyclotron radiations, *Nanomed. Nanotechnol.*, **3(2)**, 000138.

152. Heidari, A. (2018) Homonuclear correlation experiments such as homonuclear single–quantum correlation spectroscopy (HSQC), homonuclear multiple–quantum correlation spectroscopy (HMQC) and homonuclear multiple–bond correlation spectroscopy (HMBC) comparative study on malignant and benign human cancer cells and tissues under synchrotron radiation, *Austin J. Proteomics Bioinform. & Genomics*., **5(1)**, 1024.

153. Heidari, A. (2018) Atomic force microscopy based infrared (AFM–IR) spectroscopy and nuclear resonance vibrational spectroscopy comparative study on malignant and benign human cancer cells and tissues under synchrotron radiation with the passage of time, *J. Appl. Biotechnol. Bioeng*. **5(3)**, 142–148.

154. Heidari, A. (2018) Time–dependent vibrational spectral analysis of malignant and benign human cancer cells and tissues under synchrotron radiation, *J. Cancer Oncol*, **2(2)**, 000124.

155. Heidari, A. (2018) Palauamine and olympiadane nano molecules incorporation into the nano polymeric matrix (NPM) by immersion of the nano polymeric modified electrode (NPME) as molecular enzymes and drug targets for human cancer cells, tissues and tumors treatment under synchrotron and synchrocyclotron radiations, *Arc. Org. Inorg. Chem. Sci*., **3(1)**.

156. Gobato, R., Heidari, A. (2018) Infrared spectrum and sites of action of sanguinarine by molecular mechanics and ab initio methods, *International Journal of Atmospheric and Oceanic Sciences*. **2(1)**, 1–9.

157. Heidari, A. (2018) Angelic acid, diabolic acids, draculin and miraculin nano molecules incorporation into the nano polymeric matrix (NPM) by immersion of the nano polymeric modified electrode (NPME) as molecular enzymes and drug targets for human cancer cells, tissues and tumors treatment under synchrotron and synchrocyclotron radiations, *Med. & Analy. Chem. Int. J.*, **2(1)**, 000111.

158. Heidari, A. (2018) Gamma linolenic methyl ester, 5–heptadeca–5,8,11–trienyl 1,3,4–oxadiazole–2–thiol, sulphoquinovosyl diacyl glycerol, ruscogenin, nocturnoside B, protodioscine B, parquisoside–B, leiocarposide, narangenin, 7–methoxy hespertin, lupeol, rosemariquinone, rosmanol and rosemadiol nano molecules incorporation into the nano polymeric matrix (NPM) by immersion of the nano polymeric modified electrode (NPME) as molecular enzymes and drug targets for human cancer cells, tissues and tumors treatment under synchrotron and synchrocyclotron radiations, *Int. J. Pharma. Anal. Acta*, **2(1)**, 7–14.

159. Heidari, A. (2018) Fourier transform infrared (FTIR) spectroscopy, attenuated total reflectance Fourier transform infrared (ATR–FTIR) spectroscopy, micro–attenuated total reflectance Fourier transform infrared (Micro–ATR–FTIR) spectroscopy, macro–attenuated total reflectance Fourier transform infrared (Macro–ATR–FTIR) spectroscopy, two–dimensional infrared correlation spectroscopy, linear two–dimensional infrared spectroscopy, non–linear two–dimensional infrared spectroscopy, atomic force microscopy based infrared (AFM–IR) spectroscopy, infrared photodissociation spectroscopy, infrared correlation table spectroscopy, near–infrared spectroscopy (NIRS), mid–infrared spectroscopy (MIRS), nuclear resonance vibrational spectroscopy, thermal infrared spectroscopy and photothermal infrared spectroscopy comparative study on malignant and benign human cancer cells and tissues under synchrotron radiation with the passage of time, *Glob Imaging Insights*, **3(2)**, 1–14.

160. Heidari, A. (2018) Heteronuclear single–quantum correlation spectroscopy (HSQC) and heteronuclear multiple–bond correlation spectroscopy (HMBC) comparative study on malignant and benign human cancer cells, tissues and tumors under synchrotron and synchrocyclotron radiations, *Chronicle of Medicine and Surgery* **2(3)**, 144–156.

161. Heidari, A. (2018) Tetrakis [3, 5–bis (trifluoromethyl) phenyl] borate (BARF)–enhanced precatalyst preparation stabilization and initiation (EPPSI) nano molecules, *Medical Research and Clinical Case Reports* **2(1)**, 113–126.

162. Heidari, A. (2018) Sydnone, münchnone, montréalone, mogone, montelukast, quebecol and palau'amine–enhanced precatalyst preparation stabilization and initiation (EPPSI) nano molecules, *Sur. Cas. Stud. Op. Acc. J.*, **1(3)**.

163. Heidari, A. (2018) Fornacite, orotic acid, rhamnetin, sodium ethyl xanthate (SEX) and spermine (spermidine or polyamine) nano-molecules incorporation into the nanopolymeric matrix (NPM), *International Journal of Biochemistry and Biomolecules*, **4(1)**, 1–19.

164. Heidari, A. Gobato, R. (2018) Putrescine, cadaverine, spermine and spermidine–enhanced precatalyst preparation stabilization and initiation (EPPSI) nano molecules, *Parana Journal of Science and Education (PJSE)*, **4(5)**, 1–14.

165. Heidari, A. (2018) Cadaverine (1,5–pentanediamine or pentamethylenediamine), diethyl azodicarboxylate (DEAD or DEADCAT) and putrescine (tetramethylenediamine) nano molecules incorporation into the nano polymeric matrix (NPM) by immersion of the nano polymeric modified electrode (NPME) as molecular enzymes and drug targets for human cancer cells, tissues and tumors treatment under synchrotron and synchrocyclotron radiations, *Hiv and Sexual Health Open Access Open Journal*. **1(1)**, 4–11.

166. Heidari, A. (2018) Improving the performance of nano–endofullerenes in polyaniline nanostructure–based biosensors by covering californium colloidal nanoparticles with multi–walled carbon nanotubes, *Journal of Advances in Nanomaterials*, **3(1)**, 1–28.

167. Gobato, R., Haidari, A. (2018) Molecular mechanics and quantum chemical study on sites of action of sanguinarine using vibrational spectroscopy based on molecular mechanics and quantum chemical calculations, *Malaysian Journal of Chemistry*, **20(1)**, 1–23.

168. Heidari, A. (2018) Vibrational biospectroscopic studies on anti–cancer nanopharmaceuticals (Part I), *Malaysian Journal of Chemistry*, **20(1)**, 33–73.

169. Heidari, A. (2018) Vibrational biospectroscopic studies on anti–cancer nanopharmaceuticals (Part

II), *Malaysian Journal of Chemistry*, **20(1)**, 74–117.

170. Heidari, A. (2018) Uranocene ($U(C_8H_8)_2$) and bis(Cyclooctatetraene)iron ($Fe(C_8H_8)_2$ or $Fe(COT)_2$)–enhanced precatalyst preparation stabilization and initiation (EPPSI) nano molecules, *Chemistry Reports*, **1(2)**, 1–16.

171. Heidari, A. (2018) Biomedical systematic and emerging technological study on human malignant and benign cancer cells and tissues biospectroscopic analysis under synchrotron radiation, *Glob Imaging Insights*, **3(3)**, 1–7.

172. Heidari, A. (2018) Deep–level transient spectroscopy and x–ray photoelectron spectroscopy (XPS) comparative study on malignant and benign human cancer cells and tissues with the passage of time under synchrotron radiation, *Res. Dev. Material Sci*., **7(2)**, RDMS.000659.

173. Heidari, A. (2018) C70–carboxyfullerenes nano molecules incorporation into the nano polymeric matrix (NPM) by immersion of the nano polymeric modified electrode (NPME) as molecular enzymes and drug targets for human cancer cells, tissues and tumors treatment under synchrotron and synchrocyclotron radiations, *Glob Imaging Insights*, **3(3)**, 1–7.

174. Heidari, A. (2018) The effect of temperature on cadmium oxide (CdO) nanoparticles produced by synchrotron radiation in the human cancer cells, tissues and tumors, *International Journal of Advanced Chemistry*, **6(2)**, 140–156.

175. Heidari, A. (2018) A clinical and molecular pathology investigation of correlation spectroscopy (COSY), exclusive correlation spectroscopy (ECOSY), total correlation spectroscopy (TOCSY), heteronuclear single–quantum correlation spectroscopy (HSQC) and heteronuclear multiple–bond correlation spectroscopy (HMBC) comparative study on malignant and benign human cancer cells, tissues and tumors under synchrotron and synchrocyclotron radiations using cyclotron versus synchrotron, synchrocyclotron and the large hadron collider (LHC) for delivery of proton and helium ion (charged particle) beams for oncology radiotherapy, *European Journal of Advances in Engineering and Technology*, **5(7)**, 414–426.

176. Heidari, A. (2018) Nano molecules incorporation into the nano polymeric matrix (NPM) by immersion of the nano polymeric modified electrode (NPME) as molecular enzymes and drug targets for human cancer cells, tissues and tumors treatment under synchrotron and synchrocyclotron radiations, *J. Oncol Res.*, **1(1)**, 1–20.

177. Heidari, A. (2018) Use of molecular enzymes in the treatment of chronic disorders, *Canc. Oncol Open Access J*., **1(1)**, 12–15.

178. Heidari, A. (2018) Vibrational biospectroscopic study and chemical structure analysis of unsaturated polyamides nanoparticles as anti–cancer polymeric nanomedicines using synchrotron radiation, *International Journal of Advanced Chemistry*, **6(2)**, 167–189.

179. Heidari, A. (2018) Adamantane, irene, naftazone and pyridine–enhanced precatalyst preparation stabilization and initiation (PEPPSI) nano molecules, *Madridge J. Nov. Drug Res*., **2(1)**, 61–67.

180. Heidari, A. (2018) Heteronuclear single–quantum correlation spectroscopy (HSQC) and heteronuclear multiple–bond correlation spectroscopy (HMBC) comparative study on malignant and benign human cancer cells and tissues with the passage of time under synchrotron radiation, *Madridge J. Nov. Drug Res.*, **2(1)**, 68–74.

181. Heidari, A., Gobato, R. (2018) A novel approach to reduce toxicities and to improve bioavailabilities of DNA/RNA of human cancer cells–containing cocaine (Coke), lysergide (lysergic acid diethyl amide or LSD), Δ^9–tetrahydrocannabinol (THC) [(–)–trans–Δ^9–tetrahydrocannabinol], theobromine (xantheose), caffeine, aspartame (APM) (nutrasweet) and zidovudine (ZDV) [azidothymidine (AZT)] as anti–cancer nano drugs by coassembly of dual anti–cancer nano drugs to inhibit DNA/RNA of human cancer cells drug resistance, *Parana Journal of Science and Education*, **4(6)**, 1–17.

182. Heidari, A., Gobato, R. (2018) Ultraviolet photoelectron spectroscopy (UPS) and ultraviolet–visible (UV–Vis) spectroscopy comparative study on malignant and benign human cancer cells and tissues with the passage of time under synchrotron radiation, *Parana Journal of Science and Education*, **4(6)**, 18–33.

183. Gobato, R., Heidari, A., Mitra A. (2018) The creation of $C_{13}H_{20}BeLi_2SeSi$. the proposal of a bio–inorganic molecule, using ab initio methods for the genesis of a nano membrane, *Arc Org. Inorg. Chem. Sci.*, **3(4)**, AOICS.MS.ID.000167.

184. Gobato, R., Heidari, A., Mitra A. (2018) Using the quantum chemistry for genesis of a nano biomembrane with a combination of the elements

Be, Li, Se, Si, C and H, *ResearchGate*, See discussions, stats, and author profiles for this publication at https://www.researchgate.net/publication/326201181.

185. Gobato, R., Heidari, A. (2018) Using the quantum chemistry for genesis of a nano biomembrane with a combination of the elements Be, Li, Se, Si, C and H, *J. Nanomed. Res*., **7(4)**, 241–252.

186. Heidari, A. (2018) Bastadins and bastaranes–enhanced precatalyst preparation stabilization and initiation (EPPSI) nano molecules, *Glob Imaging Insights*, **3(4)**, 1–7.

187. Heidari, A. (2018) Fucitol, pterodactyladiene, DEAD or DEADCAT (diEthyl azodicarboxylate), skatole, the nanoPutians, thebacon, pikachurin, tie fighter, spermidine and mirasorvone nano molecules incorporation into the nano polymeric matrix (NPM) by immersion of the nano polymeric modified electrode (NPME) as molecular enzymes and drug targets for human cancer cells, tissues and tumors treatment under synchrotron and synchrocyclotron radiations, *Glob Imaging Insights*, **3(4)**, 1–8.

188. Dadvar, E., Heidari, A. (2018) A review on separation techniques of graphene oxide (GO)/base on hybrid polymer membranes for eradication of dyes and oil compounds: Recent progress in graphene oxide (GO)/base on polymer membranes–related nanotechnologies, *Clin. Med. Rev. Case Rep.*, **5**, 228.

189. Heidari, A., Gobato, R. (2018) First–time simulation of deoxyuridine monophosphate (dUMP) (deoxyuridylic acid or deoxyuridylate) and vomitoxin (deoxynivalenol (DON)) ((3α,7α)–3,7,15–trihydroxy–12,13–epoxytrichothec–9–en–8–one)–enhanced precatalyst preparation stabilization and initiation (EPPSI) nano molecules incorporation into the nano polymeric matrix (NPM) by immersion of the nano polymeric modified electrode (NPME) as molecular enzymes and drug targets for human cancer cells, tissues and tumors treatment under synchrotron and synchrocyclotron radiations, *Parana Journal of Science and Education*, **4(6)**, 46–67.

190. Heidari, A. (2018) Buckminsterfullerene (fullerene), bullvalene, dickite and josiphos ligands nano molecules incorporation into the nano polymeric matrix (NPM) by immersion of the nano polymeric modified electrode (NPME) as molecular enzymes and drug targets for human hematology and thromboembolic diseases prevention, diagnosis and treatment under synchrotron and synchrocyclotron radiations, *Glob Imaging Insights*, **3(4)**, 1–7.

191. Heidari, A. (2018) Fluctuation x–ray scattering (FXS) and wide–angle x–ray scattering (WAXS) comparative study on malignant and benign human cancer cells and tissues under synchrotron radiation, *Glob Imaging Insights*, **3(4)**, 1–7.

192. Heidari, A. (2018) A novel approach to correlation spectroscopy (COSY), exclusive correlation spectroscopy (ECOSY), total correlation spectroscopy (TOCSY), incredible natural–abundance double–quantum transfer experiment (INADEQUATE), heteronuclear single–quantum correlation spectroscopy (HSQC), heteronuclear multiple–bond correlation spectroscopy (HMBC), nuclear overhauser effect spectroscopy (NOESY) and rotating frame nuclear Overhauser effect spectroscopy (ROESY) comparative study on malignant and benign human cancer cells and tissues under synchrotron radiation, *Glob Imaging Insights*, **3(5)**, 1–9.

193. Heidari, A. (2018) Terphenyl–based reversible receptor with rhodamine, rhodamine–based molecular probe, rhodamine–based using the spirolactam ring opening, rhodamine B with ferrocene substituent, calix[4]arene–based receptor, thioether + aniline–derived ligand framework linked to a fluorescein platform, mercuryfluor–1 (flourescent probe), N,N'–dibenzyl–1,4,10,13–tetraraoxa–7,16–diazacyclo-octadecane and terphenyl–based reversible receptor with pyrene and quinoline as the fluorophores–enhanced precatalyst preparation stabilization and initiation (EPPSI) nano molecules, *Glob Imaging Insights*, **3(5)**, 1–9.

194. Heidari, A. (2018) Small–angle x–ray scattering (SAXS), ultra–small angle x–ray scattering (USAXS), fluctuation x–ray scattering (FXS), wide–angle x–ray scattering (WAXS), grazing–incidence small–angle x–ray scattering (GISAXS), grazing–incidence wide–angle x–ray scattering (GIWAXS), small–angle neutron scattering (SANS), grazing–incidence small–angle neutron scattering (GISANS), x–ray diffraction (XRD), powder x–ray diffraction (PXRD), wide–angle x–ray diffraction (WAXD), grazing–incidence x–ray diffraction (GIXD) and energy–dispersive x–ray diffraction (EDXRD) comparative study on malignant and benign human cancer cells and tissues under synchrotron radiation, *Glob Imaging Insights*, **3(5)**, 1–10.

195. Heidari, A. (2018) Nuclear resonant inelastic x–ray scattering spectroscopy (NRIXSS) and nuclear

resonance vibrational spectroscopy (NRVS) comparative study on malignant and benign human cancer cells and tissues under synchrotron radiation, *Glob Imaging Insights*, **3(5)**, 1–7.

196. Heidari, A. (2018) Small–angle x–ray scattering (SAXS) and ultra–small angle x–ray scattering (USAXS) comparative study on malignant and benign human cancer cells and tissues under synchrotron radiation, *Glob Imaging Insights*, **3(5)**, 1–7.

197. Heidari, A. (2018) Curious chloride ($CmCl_3$) and titanic chloride ($TiCl_4$)–enhanced precatalyst preparation stabilization and initiation (EPPSI) nano molecules for cancer treatment and cellular therapeutics, *J. Cancer Research and Therapeutic Interventions*, **1(1)**, 01–10.

198. Gobato, R., Gobato, M. R. R., Heidari, A., Mitra, A. (2018) Spectroscopy and dipole moment of the molecule $C_{13}H_{20}BeLi_2SeSi$ via quantum chemistry using ab initio, Hartree–Fock method in the base set CC–pVTZ and 6–311G**(3df, 3pd), *Arc. Org. Inorg. Chem. Sci.*, **3(5)**, 402–409.

199. Heidari, A. (2018) C_{60} and C_{70}–encapsulating carbon nanotubes incorporation into the nano polymeric matrix (NPM) by immersion of the nano polymeric modified electrode (NPME) as molecular enzymes and drug targets for human cancer cells, tissues and tumors treatment under synchrotron and synchrocyclotron radiations, *Integr. Mol. Med.*, **5(3)**, 1–8.

200. Heidari, A. (2018) Two–dimensional (2D) ^{1}H or proton NMR, ^{13}C NMR, ^{15}N NMR and ^{31}P NMR spectroscopy comparative study on malignant and benign human cancer cells and tissues under synchrotron radiation with the passage of time, *Glob Imaging Insights*, **3(6)**, 1–8.

201. Heidari, A. (2018) FT–Raman spectroscopy, coherent anti–stokes Raman spectroscopy (CARS) and Raman optical activity spectroscopy (ROAS) comparative study on malignant and benign human cancer cells and tissues with the passage of time under synchrotron radiation, *Glob Imaging Insights*, **3(6)**, 1–8.

202. Heidari, A. (2018) A modern and comprehensive investigation of inelastic electron tunneling spectroscopy (IETS) and scanning tunneling spectroscopy on malignant and benign human cancer cells, tissues and tumors through optimizing synchrotron microbeam radiotherapy for human cancer treatments and diagnostics: An experimental biospectroscopic comparative study, *Glob Imaging Insights*, **3(6)**, 1–8.

203. Heidari, A. (2018) A hypertension approach to thermal infrared spectroscopy and photothermal infrared spectroscopy comparative study on malignant and benign human cancer cells and tissues under synchrotron radiation with the passage of time, *Glob Imaging Insights*, **3(6)**, 1–8.

204. Heidari, A. (2018) Incredible natural–abundance double–quantum transfer experiment (INADEQUATE), nuclear Overhauser effect spectroscopy (NOESY) and rotating frame nuclear Overhauser effect spectroscopy (ROESY) comparative study on malignant and benign human cancer cells and tissues under synchrotron radiation, *Glob Imaging Insights*, **3(6)**, 1–8.

205. Heidari, A. (2018) 2–amino–9–((1S, 3R, 4R)–4–hydroxy–3–(hydroxymethyl)–2–methylenecyclopentyl)–1H–purin–6(9H)–one, 2–amino–9–((1R, 3R, 4R)–4–hydroxy–3–(hydroxymethyl)–2–methylenecyclopentyl)–1H–purin–6(9H)–one, 2–amino–9–((1R, 3R, 4S)–4–hydroxy–3–(hydroxymethyl)–2–methylenecyclopentyl)–1H–purin–6(9H)–one and 2–amino–9–((1S, 3R, 4S)–4–hydroxy–3–(hydroxymethyl)–2–methylenecyclopentyl)–1H–purin–6(9H)–one–enhanced precatalyst preparation stabilization and initiation nano molecules, *Glob Imaging Insights*, **3(6)**, 1–9.

206. Gobato, R., Gobato, M. R. R., Heidari, A., Mitra, A. (2018) Spectroscopy and dipole moment of the molecule $C_{13}H_{20}BeLi_2SeSi$ via quantum chemistry using ab initio, Hartree–Fock method in the base set CC–pVTZ and 6–311G**(3df, 3pd), *American Journal of Quantum Chemistry and Molecular Spectroscopy*, **2(1)**, 9–17.

207. Heidari, A. (2018) Production of electrochemiluminescence (ECL) biosensor using Os–Pd/HfC nanocomposites for detecting and tracking of human gastroenterological cancer cells, tissues and tumors, *Int J Med Nano Res* **5(1)**, 22–34.

208. Heidari, A. (2018) Enhancing the Raman scattering for diagnosis and treatment of human cancer cells, tissues and tumors using cadmium oxide (CdO) nanoparticles, *J. Toxicol. Risk Assess*, **4(1)**, 12–25.

209. Heidari, A. (2018) Human malignant and benign human cancer cells and tissues biospectroscopic analysis under synchrotron radiation using anti–cancer nano drugs delivery, *Integr. Mol. Med.*, **5(5)**, 1–13.

210. Heidari, A. (2018) Analogous nano compounds of the form $M(C_8H_8)_2$ exist for M = (Nd, Tb, Pu, Pa, Np, Th, and Yb)–enhanced precatalyst preparation stabilization and initiation (EPPSI) nano molecules, *Integr. Mol. Med.*, **5(5)**, 1–8.

211. Heidari, A. (2018) Hadron spectroscopy, baryon spectroscopy and meson spectroscopy comparative study on malignant and benign human cancer cells and tissues under synchrotron radiation, *Integr. Mol. Med.*, **5(5)**, 1–8.

212. Gobato, R., Gobato, M. R. R., Heidari, A. (2019) Raman spectroscopy study of the nano molecule $C_{13}H_{20}BeLi_2SeSi$ using ab initio and Hartree–Fock methods in the basis set CC–pVTZ and 6–311G** (3df, 3pd), *International Journal of Advanced Engineering and Science*, **7(1)**, 14–35.

213. Heidari, A., Gobato, R. (2019) Evaluating the effect of anti–cancer nano drugs dosage and reduced leukemia and polycythemia vera levels on trend of the human blood and bone marrow cancers under synchrotron radiation, *Trends in Res.*, **2(1)**, 1–8.

214. Heidari, A., Gobato, R. (2019) Assessing the variety of synchrotron, synchrocyclotron and LASER radiations and their roles and applications in human cancer cells, tissues and tumors diagnosis and treatment, *Trends in Res.*, **2(1)**, 1–8.

215. Heidari, A., Gobato, R. (2019) Pros and cons controversy on malignant human cancer cells, tissues and tumors transformation process to benign human cancer cells, tissues and tumors, *Trends in Res.*, **2(1)**, 1–8.

216. Heidari, A., Gobato, R. (2019) Three–dimensional (3D) simulations of human cancer cells, tissues and tumors for using in human cancer cells, tissues and tumors diagnosis and treatment as a powerful tool in human cancer cells, tissues and tumors research and anti–cancer nano drugs sensitivity and delivery area discovery and evaluation, *Trends in Res.*, **2(1)**, 1–8.

217. Heidari, A., Gobato, R. (2019) Investigation of energy production by synchrotron, synchro-cyclotron and LASER radiations in human cancer cells, tissues and tumors and evaluation of their effective on human cancer cells, tissues and tumors treatment trend, *Trends in Res.*, **2(1)**, 1–8.

218. Heidari, A., Gobato, R. (2019) High–resolution mapping of DNA/RNA hypermethylation and hypomethylation process in human cancer cells, tissues and tumors under synchrotron radiation, *Trends in Res.*, **2(2)**, 1–9.

219. Heidari, A. (2019) A novel and comprehensive study on manufacturing and fabrication nano-particles methods and techniques for processing cadmium oxide (CdO) nanoparticles colloidal solution, *Glob Imaging Insights*, **4(1)**, 1–8.

220. Heidari, A. (2019) A combined experimental and computational study on the catalytic effect of aluminum nitride nanocrystal (AlN) on the polymerization of benzene, naphthalene, anthracene, phenanthrene, chrysene and tetracene, *Glob Imaging Insights*, **4(1)**, 1–8.

221. Heidari, A. (2019) Novel experimental and three–dimensional (3D) multiphysics computational framework of michaelis–menten kinetics for catalyst processes innovation, characterization and carrier applications, *Glob Imaging Insights*, **4(1)**, 1–8.

222. Heidari, A. (2019) The hydrolysis constants of copper (I) (Cu^+) and copper (II) (Cu^{2+}) in aqueous solution as a function of pH using a combination of pH measurement and biospectroscopic methods and techniques, *Glob Imaging Insights*, **4(1)**, 1–8.

223. Heidari, A. (2019) Vibrational biospectroscopic study of ginormous virus–sized macromolecule and polypeptide macromolecule as mega macromolecules using attenuated total reflectance–Fourier transform infrared (ATR–FTIR) spectroscopy and Mathematica 11.3, *Glob Imaging Insights*, **4(1)**, 1–8.

224. Heidari, A. (2019) Three–dimensional (3D) imaging spectroscopy of carcinoma, sarcoma, leukemia, lymphoma, multiple myeloma, melanoma, brain and spinal cord tumors, germ cell tumors, neuroendocrine tumors and carcinoid tumors under synchrotron radiation, *Glob Imaging Insights*, **4(1)**, 1–9.

225. Gobato, R., Gobato, M. R. R., Heidari, A. (2019) Storm vortex in the center of paraná state on June 6, 2017: A case study, *Sumerianz Journal of Scientific Research*, **2(2)**, 24–31.

226. Gobato, R., Gobato, M. R. R., Heidari, A. (2019) Attenuated total reflection–Fourier transform infrared (ATR–FTIR) spectroscopy study of the nano molecule $C_{13}H_{20}BeLi_2SeSi$ using ab initio and Hartree–Fock methods in the basis set RHF/CC–pVTZ and RHF/6–311G** (3df, 3pd): An experimental challenge to chemists, *Chemistry Reports*, **2(1)**, 1–26.

227. Heidari, A. (2019) Three–dimensional (3D) imaging spectroscopy of carcinoma, sarcoma, leukemia, lymphoma, multiple myeloma, melanoma, brain and spinal cord tumors, germ cell tumors, neuroendocrine tumors and carcinoid tumors under synchrocyclotron radiation, *Res Adv Biomed Sci Technol* **1(1)**, 01–17.

228. Gobato, R., Gobato, M. R. R., Heidari, A., Mitra A. (2019) New nano–molecule kurumi–$C_{13}H_{20}BeLi_2SeSi/C_{13}H_{19}BeLi_2SeSi$, and Raman spectroscopy using ab initio, Hartree–Fock method in the base set CC–pVTZ and 6–311G** (3df, 3pd), *J. Anal. Pharm. Res*., **8(1)**, 1–6.

229. Heidari, A., Esposito, J., Caissutti, A. (2019) The importance of attenuated total reflectance Fourier transform infrared (ATR–FTIR) and Raman bio-spectroscopy of single–walled carbon nanotubes (SWCNT) and multi–walled carbon nanotubes (MWCNT) in interpreting infrared and Raman spectra of human cancer cells, tissues and tumors, *Oncogen* **2(2)**, 1–21.

230. Heidari, A. (2019) Mechanism of action and their side effects at a glance prevention, treatment and management of immune system and human cancer nano chemotherapy, *Nanosci. Technol.,* **6(1)**, 1–4.

231. Heidari, A., Esposito, J., Caissutti, A. (2019) The quantum entanglement dynamics induced by non–linear interaction between a moving nano molecule and a two–mode field with two–photon transitions using reduced Von Neumann entropy and Jaynes–Cummings model for human cancer cells, tissues and tumors diagnosis, *Int. J. Crit. Care Emerg. Med.,* **5(2)**, 071–084.

232. Heidari, A., Esposito, J., Caissutti, A. (2019) Palytoxin time–resolved absorption and resonance FT–IR and Raman biospectroscopy and density functional theory (DFT) investigation of vibronic–mode coupling structure in vibrational spectra analysis, *J. Pharm. Drug Res.,* **3(1)**, 150–170.

233. Heidari, A., Esposito, J., Caissutti, A. (2019) Aplysiatoxin time–resolved absorption and resonance FT–IR and Raman biospectroscopy and density functional theory (DFT) investigation of vibronic–mode coupling structure in vibrational spectra analysis, *J. Chem. Sci. Eng.*, **2(2)**, 70–89.

234. Gobato, R., Gobato, M. R. R., Heidari, A., Mitra, A. (2018) Spectroscopy and dipole moment of the molecule $C_{13}H_{20}BeLi_2SeSi$ via quantum chemistry using ab initio, Hartree–Fock method in the base set CC–pVTZ and 6–311G** (3df, 3pd), *American Journal of Quantum Chemistry and Molecular Spectroscopy*, **2(1)**, 9–17.

235. Heidari, A., Esposito, J., Caissutti, A. (2019) Cyanotoxin time–resolved absorption and resonance FT–IR and Raman biospectroscopy and density functional theory (DFT) investigation of vibronic–mode coupling structure in vibrational spectra analysis, *Br. J. Med. Health Res*., **6(4)**, 21–60.

236. Heidari, A. (2019) Potential and theranostics applications of novel anti–cancer nano drugs delivery systems in preparing for clinical trials of synchrotron microbeam radiation therapy (SMRT) and synchrotron stereotactic radiotherapy (SSRT) for treatment of human cancer cells, tissues and tumors using image guided synchrotron radiotherapy (IGSR), *Ann. Nanosci. Nanotechnol*., **3(1)**, 1006–1019.

237. Heidari, A., Esposito, J., Caissutti, A. (2019) Study of anti–cancer properties of thin layers of cadmium oxide (CdO) nanostructure, *Int. J. Analyt. Bioanalyt. Methods,* **1(1)**, 3–22.

238. Heidari, A., Esposito, J., Caissutti, A. (2019) Alpha–conotoxin, omega–conotoxin and mu–conotoxin time–resolved absorption and resonance FT–IR and Raman biospectroscopy and density functional theory (DFT) investigation of vibronic–mode coupling structure in vibrational spectra analysis, *International Journal of Advanced Chemistry*, **7(1)**, 52–66.

239. Heidari, A. (2019) Clinical and medical pros and cons of human cancer cells' enzymotherapy, immunotherapy, chemotherapy, radiotherapy, hormone therapy and targeted therapy process under synchrotron radiation: A case study on mechanism of action and their side effects, *Parana Journal of Science and Education (PJSE)*, **5(3)**, 1–23.

240. Heidari, A. (2019) The importance of the power in CMOS inverter circuit of synchrotron and synchrocyclotron radiations using 50 (nm) and 100 (nm) technologies and reducing the voltage of power supply, *Radiother Oncol Int*., **1(1)**, 1002–1015.

241. Heidari, A., Esposito, J., Caissutti, A. (2019) The importance of quantum hydrodynamics (QHD) approach to single–walled carbon nanotubes (SWCNT) and multi–walled carbon nanotubes (MWCNT) in genetic science, *SCIOL Genet. Sci*., **2(1)**, 113–129.

242. Heidari, A., Esposito, J., Caissutti, A. (2019)

Anatoxin–a and anatoxin–a(s) time–resolved absorption and resonance FT–IR and Raman biospectroscopy and density functional theory (DFT) investigation of vibronic–mode coupling structure in vibrational spectra analysis, *Saudi J. Biomed. Res.*, **4(4)**, 174–194.

243. Gobato, R., Gobato, M. R. R., Heidari, A. (2019) Evidence of tornado storm hit the counties of Rio Branco do Ivaí and Rosario de Ivaí, Southern Brazil, *Sci. Lett.*, **7(1)**, 32–40.

244. Jeyaraj, M., Mahalingam, V., Indhuleka, A., Sennu, P., Ho, M.S., Heidari A. (2019) Chemical analysis of surface water quality of river Noyyal connected tank in Tirupur district, Tamil Nadu, India, *Water and Energy International*, **62(1)**, 63–68.

245. Heidari, A., Esposito, J., Caissutti, A. (2019) 6–methoxy–8–[[6–methoxy–8–[[6–methoxy–2–methyl–1–(2–methylpropyl)–3,4–dihydro–1H–isoquinolin–7–yl]oxy]–2–methyl–1–(2–methyl-propyl)–3,4–dihydro–1H–isoquinolin–7–yl]oxy]–2–methyl–1–(2–methylpropyl)–3,4–dihydro–1H–isoquinolin–7–ol time–resolved absorption and resonance FT–IR and Raman biospectroscopy and density functional theory (DFT) investigation of vibronic–mode coupling structure in vibrational spectra analysis, *J. Adv. Phys. Chem.*, **1(1)**, 1–6.

246. Heidari, A., Esposito, J., Caissutti, A. (2019) Shiga toxin and shiga–like toxin (SLT) time–resolved absorption and resonance FT–IR and Raman biospectroscopy and density functional theory (DFT) investigation of vibronic–mode coupling structure in vibrational spectra analysis, *Annal. Biostat. & Biomed. Appli*., **2(3)**, 1–4.

247. Heidari, A., Esposito, J., Caissutti, A. (2019) Alpha–bungarotoxin, beta–bungarotoxin and kappa–bungarotoxin time–resolved absorption and resonance FT–IR and Raman biospectroscopy and density functional theory (DFT) investigation of vibronic–mode coupling structure in vibrational spectra analysis, Archives of Pharmacology and Pharmaceutical Sciences, *ReDelve*, **2019(1)**, 1–24.

248. Heidari, A., Esposito, J., Caissutti, A. (2019) Okadaic acid time–resolved absorption and resonance FT–IR and Raman biospectroscopy and density functional theory (DFT) investigation of vibronic–mode coupling structure in vibrational spectra analysis, *Int. J. Analyt. Bioanalyt. Methods*, **1(1)**, 1–19.

249. Heidari A. (2019) Investigation of the processes of absorption, distribution, metabolism and elimination (ADME) as vital and important factors for modulating drug action and toxicity, *Open Access J. Oncol*, **2(1)**, 180010–180012.

250. Heidari, A., Esposito, J., Caissutti, A. (2019) Pertussis toxin time–resolved absorption and resonance FT–IR and Raman biospectroscopy and density functional theory (DFT) investigation of vibronic–mode coupling structure in vibrational spectra analysis, *Chemistry Reports*, **1(2)**, 1–5.

251. Gobato, R., Gobato, M.R.R., Heidari, A. (2019) Rhodochrosite as crystal oscillator, *Am. J. Biomed. Sci. & Res*., **3(2)**, 187.

252. Heidari, A., Esposito, J., Caissutti, A. (2019) Tetrodotoxin (TTX) time–resolved absorption and resonance FT–IR and Raman biospectroscopy and density functional theory (DFT) investigation of vibronic–mode coupling structure in vibrational spectra analysis, *Journal of New Developments in Chemistry*, **2(3)**, 26–48.

253. Heidari, A., Esposito, J., Caissutti, A. (2019) The importance of analysis of vibronic–mode coupling structure in vibrational spectra of supramolecular aggregates of (CA*M) cyanuric acid (CA) and melamine (M) beyond the Franck–Condon approximation, *Journal of Clinical and Medical Images*, **2(2)**, 1–20.

254. Heidari, A., Esposito, J., Caissutti, A. (2019) Microcystin–LR time–resolved absorption and resonance FT–IR and Raman biospectroscopy and density functional theory (DFT) investigation of vibronic–mode coupling structure in vibrational spectra analysis, *Malaysian Journal of Chemistry*, **21(1)**, 70–95.

255. Heidari, A., Esposito, J., Caissutti, A. (2019) Botulinum toxin time–resolved absorption and resonance FT–IR and Raman biospectroscopy and density functional theory (DFT) investigation of vibronic–mode coupling structure in vibrational spectra analysis, *Journal of Mechanical Design and Vibration*, **7(1)**, 1–15.

256. Heidari, A., Esposito, J., Caissutti, A. (2019) Domoic acid (DA) time–resolved absorption and resonance FT–IR and Raman biospectroscopy and density functional theory (DFT) investigation of vibronic–mode coupling structure in vibrational spectra analysis, *Cientific Clinical Oncology Journal* **1(2)**, 03–07.

257. Heidari, A., Esposito, J., Caissutti, A. (2019) Surugatoxin (SGTX) time–resolved absorption and resonance FT–IR and Raman biospectroscopy

and density functional theory (DFT) investigation of vibronic–mode coupling structure in vibrational spectra analysis, *Cientific Clinical Oncology Journal*, **1(2)**, 14–18.

258. Heidari, A., Esposito, J., Caissutti, A. (2019) Decarbamoylsaxitoxin time–resolved absorption and resonance FT–IR and Raman biospectroscopy and density functional theory (DFT) investigation of vibronic–mode coupling structure in vibrational spectra analysis, *Cientific Clinical Oncology Journal*, **1(2)**, 19–23.

259. Heidari, A., Esposito, J., Caissutti, A. (2019) Gonyautoxin (GTX) time–resolved absorption and resonance FT–IR and Raman biospectroscopy and density functional theory (DFT) investigation of vibronic–mode coupling structure in vibrational spectra analysis, *Cientific Clinical Oncology Journal*, **1(2)**, 24–28.

260. Heidari, A., Esposito, J., Caissutti, A. (2019) Hislrionicotoxin time–resolved absorption and resonance FT–IR and Raman biospectroscopy and density functional theory (DFT) investigation of vibronic–mode coupling structure in vibrational spectra analysis, *Cientific Drug Delivery Research* **1(1)**, 01–06.

261. Heidari, A., Esposito, J., Caissutti, A. (2019) Dihydrokainic acid time–resolved absorption and resonance FT–IR and Raman biospectroscopy and density functional theory (DFT) investigation of vibronic–mode coupling structure in vibrational spectra analysis, *Cientific Drug Delivery Research* **1(1)**, 07–12.

262. Heidari, A., Esposito, J., Caissutti, A. (2019) Aflatoxin B1 (AFB1), B2 (AFB2), G1 (AFG1), G2 (AFG2), M1 (AFM1), M2 (AFM2), Q1 (AFQ1) and P1 (AFP1) time–resolved absorption and resonance FT–IR and Raman biospectroscopy and density functional theory (DFT) investigation of vibronic–mode coupling structure in vibrational spectra analysis, *Cientific Drug Delivery Research* **1(1)**, 25–32.

263. Heidari, A., Esposito, J., Caissutti, A. (2019) Mycotoxin time–resolved absorption and resonance FT–IR and Raman biospectroscopy and density functional theory (DFT) investigation of vibronic–mode coupling structure in vibrational spectra analysis, *Cientific Drug Delivery Research* **1(1)**, 13–18.

264. Heidari, A., Esposito, J., Caissutti, A. (2019) Bufotoxin time–resolved absorption and resonance FT–IR and Raman biospectroscopy and density functional theory (DFT) investigation of vibronic–mode coupling structure in vibrational spectra analysis, *Cientific Drug Delivery Research* **1(1)**, 19–24.

265. Heidari, A., Esposito, J., Caissutti, A. (2019) Kainic acid (kainite) time–resolved absorption and resonance FT–IR and Raman biospectroscopy and density functional theory (DFT) investigation of vibronic–mode coupling structure in vibrational spectra analysis, *Cientific Journal of Neurology* **1(2)**, 02–07.

266. Heidari, A., Esposito, J., Caissutti, A. (2019) Nereistoxin time–resolved absorption and resonance FT–IR and Raman biospectroscopy and density functional theory (DFT) investigation of vibronic–mode coupling structure in vibrational spectra analysis, *Cientific Journal of Neurology* **1(2)**, 19–24.

267. Heidari, A., Esposito, J., Caissutti, A. (2019) Spider toxin and raventoxin time–resolved absorption and resonance FT–IR and Raman biospectroscopy and density functional theory (DFT) investigation of vibronic–mode coupling structure in vibrational spectra analysis, *Parana Journal of Science and Education*. **5(4)**, 1–28.

268. Heidari, A., Esposito, J., Caissutti, A. (2019) Ochratoxin A, ochratoxin B, ochratoxin C, ochratoxin α and ochratoxin TA time–resolved absorption and resonance FT–IR and Raman biospectroscopy and density functional theory (DFT) investigation of vibronic–mode coupling structure in vibrational spectra analysis, *Cientific Drug Delivery Research* **1(2)**, 03–10.

269. Heidari, A., Esposito, J., Caissutti, A. (2019) Brevetoxin A and B time–resolved absorption and resonance FT–IR and Raman biospectroscopy and density functional theory (DFT) investigation of vibronic–mode coupling structure in vibrational spectra analysis, *Cientific Drug Delivery Research* **1(2)**, 11–16.

270. Heidari, A., Esposito, J., Caissutti, A. (2019) Lyngbyatoxin–a time–resolved absorption and resonance FT–IR and Raman biospectroscopy and density functional theory (DFT) investigation of vibronic–mode coupling structure in vibrational spectra analysis, *Cientific Drug Delivery Research* **1(2)**, 23–28.

271. Heidari, A., Esposito, J., Caissutti, A. (2019) Balraechotoxin (BTX) time–resolved absorption and resonance FT–IR and Raman biospectroscopy and density functional theory (DFT) investigation

of vibronic–mode coupling structure in vibrational spectra analysis, *Cientific Journal of Neurology* **1(3)**, 1–5.

272. Heidari, A., Esposito, J., Caissutti, A. (2019) Hanatoxin time–resolved absorption and resonance FT–IR and Raman biospectroscopy and density functional theory (DFT) investigation of vibronic–mode coupling structure in vibrational spectra analysis, *Int. J. Pharm. Sci. Rev. Res.*, **57(1)**, 21–32.

273. Heidari, A., Esposito, J., Caissutti, A. (2019) Neurotoxin and alpha–neurotoxin time–resolved absorption and resonance FT–IR and Raman biospectroscopy and density functional theory (DFT) investigation of vibronic–mode coupling structure in vibrational spectra analysis, *J. Biomed. Sci. & Res*., **3(6)**, 550–563.

274. Heidari, A., Esposito, J., Caissutti, A. (2019) Antillatoxin (ATX) time–resolved absorption and resonance FT–IR and Raman biospectroscopy and density functional theory (DFT) investigation of vibronic–mode coupling structure, *American Journal of Optics and Photonics*. **7(1)**, 18–27.

275. Gobato, R., Gobato, M.R.R., Heidari, A. (2019) Calculation by UFF method of frequencies and vibrational temperatures of the unit cell of the rhodochrosite crystal, *International Journal of Advanced Chemistry*, **7(2)**, 77–81.

276. Heidari, A., Esposito, J., Caissutti, A. (2019) Analysis of vibronic–mode coupling structure in vibrational spectra of fuzeon as a 36 amino acid peptide for HIV therapy beyond the multi–dimensional Franck–Condon integrals approximation, *International Journal of Advanced Chemistry*, **7(2)**, 82–96.

277. Heidari, A., Esposito, J., Caissutti, A. (2019) Debromoaplysiatoxin time–resolved absorption and resonance FT–IR and Raman biospectroscopy and density functional theory (DFT) investigation of vibronic–mode coupling structure in vibrational spectra analysis, *Applied Chemistry*, **2(1)**, 17–54.

278. Heidari, A., Esposito, J., Caissutti, A. (2019) Enterotoxin time–resolved absorption and resonance FT–IR and Raman biospectroscopy and density functional theory (DFT) investigation of vibronic–mode coupling structure in vibrational spectra analysis, *JRL J. Sci. Technol*., **1(2)**, 1–16.

279. Gobato, R., Gobato, M.R.R., Heidari, A., Mitra, A. (2019) Rhodochrosite optical indicatrix, *Peer Res. Nest*., **1(3)**, 1–2.

280. Heidari, A., Esposito, J., Caissutti, A. (2019) Anthrax toxin time–resolved absorption and resonance FT–IR and Raman biospectroscopy and density functional theory (DFT) investigation of vibronic–mode coupling structure in vibrational spectra analysis, *Research & Reviews: Journal of Computational Biology*, **8(2)**, 23–51.

281. Heidari, A., Esposito, J., Caissutti, A. (2019) Kalkitoxin time–resolved absorption and resonance FT–IR and Raman biospectroscopy and density functional theory (DFT) investigation of vibronic–mode coupling structure in vibrational spectra analysis, *Can. J. Biomed. Res. & Tech*., **2(1)**, 1–21.

282. Heidari, A., Esposito, J., Caissutti, A. (2019) Neosaxitoxin time–resolved absorption and resonance FT–IR and Raman biospectroscopy and density functional theory (DFT) investigation of vibronic–mode coupling structure in vibrational spectra analysis, *Clin. Case Studie. Rep.*, **2(3)**, 1–14.

283. Heidari, A., Esposito, J., Caissutti, A. (2019) 6–methoxy–8–[[6–methoxy–8–[[6–methoxy–2–methyl–1–(2–methylpropyl)–3,4–dihydro–1H–isoquinolin–7–yl]oxy]–2–methyl–1–(2–methyl-propyl)–3,4–dihydro–1H–isoquinolin–7–yl]oxy]–2–methyl–1–(2–methylpropyl)–3,4–dihydro–1H–isoquinolin–7–ol time–resolved absorption and resonance FT–IR and Raman biospectroscopy and density functional theory (DFT) investigation of vibronic–mode coupling structure in vibrational spectra analysis, *Clin. Case Studie. Rep.*, **2(3)**, 1–14.

284. Heidari, A. (2019) Comparison of synchrotron radiation and synchrocyclotron radiation performance in monitoring of human cancer cells, tissues and tumors, *Clin. Case Studie. Rep.*, **2(3)**, 1–12.

285. Heidari, A., Esposito, J., Caissutti, A. (2019) Kalkitoxin time–resolved absorption and resonance FT–IR and Raman biospectroscopy and density functional theory (DFT) investigation of vibronic–mode coupling structure in vibrational spectra analysis, *Clin. Case Studie. Rep.*, **2(3)**, 1–14.

286. Heidari, A., Esposito, J., Caissutti, A. (2019) Diphtheria toxin time–resolved absorption and resonance FT–IR and Raman biospectroscopy and density functional theory (DFT) investigation of vibronic–mode coupling structure in vibrational spectra analysis: A spectroscopic study on an anti–cancer drug, *Clin. Case Studie. Rep.*, **2(3)**, 1–14.

287. Heidari, A., Esposito, J., Caissutti, A. (2019) Sym-

biodinolide time–resolved absorption and resonance FT–IR and Raman biospectroscopy and density functional theory (DFT) investigation of vibronic–mode coupling structure in vibrational spectra analysis, *Clin. Case Studie. Rep.*, **2(3)**, 1–14.

288. Heidari, A., Esposito, J., Caissutti, A. (2019) Saxitoxin time–resolved absorption and resonance FT–IR and Raman biospectroscopy and density functional theory investigation of vibronic–mode coupling structure in vibrational spectra analysis, *Am. J. Exp. Clin. Res*., **6(4)**, 364–377.

289. Gobato, R., Gobato, M.R.R., Heidari, A., Mitra, A. (2019) Hartree–Fock methods analysis protonated rhodochrosite crystal and potential in the elimination of cancer cells through synchrotron radiation, *Radiation Science and Technology*, **5(3)**, 27–36.

290. Gobato, R., Dosh, I.K.K., Heidari, A., Mitra, A., Gobato, M.R.R. (2019) Perspectives on the elimination of cancer cells using rhodochrosite crystal through synchrotron radiation, and absorption the tumoral and non–tumoral tissues, *Arch Biomed. Eng. & Biotechnol*., **3(2)**, 1–2.

291. Gobato, R., Gobato, M.R.R., Heidari, A., Mitra, A. (2019) Unrestricted Hartree–Fock computational simulation in a protonated rhodochrosite crystal, *Phys. Astron Int. J*., **3(6)**, 220–228.

292. Heidari, A., Schmitt, K., Henderson, M., Besana, E. (2019) Perspectives on sub–nanometer level of electronic structure of the synchrotron with mendelevium nanoparticles for elimination of human cancer cells, tissues and tumors treatment using Mathematica 12.0, *Journal of Energy Conservation*, **1(2)**, 46–73.

293. Heidari, A., Schmitt, K., Henderson, M., Besana, E. (2019) Simulation of interaction of synchrotron radiation emission as a function of the beam energy and bohrium nanoparticles using 3D finite element method (FEM) as an optothermal human cancer cells, tissues and tumors treatment, *Current Research in Biochemistry and Molecular Biology*, **1(1)**, 17–44.

294. Heidari, A., Schmitt, K., Henderson, M., Besana, E. (2019) Investigation of interaction between synchrotron radiation and thulium nanoparticles for human cancer cells, tissues and tumors treatment, *European Journal of Scientific Exploration*, **2(3)**, 1–8.

295. Heidari, A., Schmitt, K., Henderson, M., Besana, E. (2020) The effectiveness of the treatment human cancer cells, tissues and tumors using darmstadtium nanoparticles and synchrotron radiation, *International Journal of Advanced Engineering and Science*, **9(1)**, 9–39.

296. Heidari, A., Schmitt, K., Henderson, M., Besana, E. (2019) Using 3D finite element method (FEM) as an optothermal human cancer cells, tissues and tumors treatment in simulation of interaction of synchrotron radiation emission as a function of the beam energy and uranium nanoparticles, *Nano Prog.*, **1(2)**, 1–6.

297. Heidari, A., Schmitt, K., Henderson, M., Besana, E. (2019) A new approach to interaction between beam energy and erbium nanoparticles, *Saudi J. Biomed. Res.*, **4(11)**, 372–396.

298. Heidari, A., Schmitt, K., Henderson, M., Besana, E. (2019) Consideration of energy functions and wave functions of the synchrotron radiation and samarium nanoparticles interaction during human cancer cells, tissues and tumors treatment process, *Sci. Int. (Lahore)*, **31(6)**, 885–908.

299. Heidari, A., Schmitt, K., Henderson, M., Besana, E. (2019) An outlook on optothermal human cancer cells, tissues and tumors treatment using lanthanum nanoparticles under synchrotron radiation, *Journal of Materials Physics and Chemistry*, **7(1)**, 29–45.

300. Heidari, A., Schmitt, K., Henderson, M., Besana, E. (2019) Effectiveness of einsteinium nanoparticles in optothermal human cancer cells, tissues and tumors treatment under synchrotron radiation, *Journal of Analytical Oncology*, **8(1)**, 43–62.

301. Heidari, A., Schmitt, K., Henderson, M., Besana, E. (2019) Study of relation between synchrotron radiation and dubnium nanoparticles in human cancer cells, tissues and tumors treatment process, *Int. Res. J. Applied Sci*., **1(4)**, 1–20.

302. Heidari, A., Schmitt, K., Henderson, M., Besana, E. (2019) A novel prospect on interaction of synchrotron radiation emission and europium nanoparticles for human cancer cells, tissues and tumors treatment, *European Modern Studies Journal*, **3(5)**, 11–24.

303. Heidari, A., Schmitt, K., Henderson, M., Besana, E. (2019) Advantages, effectiveness and efficiency of using neodymium nanoparticles by 3D finite element method (FEM) as an optothermal human cancer cells, tissues and tumors treatment under synchrotron radiation, *International Journal of Advanced Chemistry*, **7(2)**, 119–135.

304. Heidari, A., Schmitt, K., Henderson, M., Besana, E. (2019) Role and applications of promethium nanoparticles in human cancer cells, tissues and tumors treatment, *Scientific Modelling and Research*, **4(1)**, 8–14.

305. Heidari, A., Esposito, J., Caissutti, A. (2019) Maitotoxin time–resolved absorption and resonance FT–IR and Raman biospectroscopy and density functional theory (DFT) investigation of vibronic–mode coupling structure in vibrational spectra analysis: A spectroscopic study on an anti–cancer drug, *Glob Imaging Insights*, **4(2)**, 1–13.

306. Heidari, A., Esposito, J., Caissutti, A. (2019) Biotoxin time–resolved absorption and resonance FT–IR and Raman biospectroscopy and density functional theory (DFT) investigation of vibronic–mode coupling structure in vibrational spectra analysis, *Glob Imaging Insights*, **4(2)**, 1–14.

307. Heidari, A., Esposito, J., Caissutti, A. (2019) Time–resolved resonance FT–IR and Raman spectroscopy and density functional theory investigation of vibronic–mode coupling structure in vibrational spectra of nanopolypeptide macromolecule beyond the multi–dimensional Franck–Condon integrals approximation and density matrix method, *Glob Imaging Insights*, **4(2)**, 1–14.

308. Heidari, A., Esposito, J., Caissutti, A. (2019) Cholera toxin time–resolved absorption and resonance FT–IR and Raman biospectroscopy and density functional theory (DFT) investigation of vibronic–mode coupling structure in vibrational spectra analysis, *Glob Imaging Insights*, **4(2)**, 1–14.

309. Heidari, A., Esposito, J., Caissutti, A. (2019) Nodularin time–resolved absorption and resonance FT–IR and Raman biospectroscopy and density functional theory (DFT) investigation of vibronic–mode coupling structure in vibrational spectra analysis, *Glob Imaging Insights*, **4(2)**, 1–14.

310. Heidari, A., Esposito, J., Caissutti, A. (2019) Cangitoxin time–resolved absorption and resonance FT–IR and Raman biospectroscopy and density functional theory (DFT) investigation of vibronic–mode coupling structure in vibrational spectra analysis, *Glob Imaging Insights*, **4(2)**, 1–13.

311. Heidari, A., Esposito, J., Caissutti, A. (2019) Ciguatoxin time–resolved absorption and resonance FT–IR and Raman biospectroscopy and density functional theory (DFT) investigation of vibronic–mode coupling structure in vibrational spectra analysis, *Glob Imaging Insights*, **4(2)**, 1–14.

312. Heidari, A., Esposito, J., Caissutti, A. (2019) Brevetoxin (a) and (b) time–resolved absorption and resonance FT–IR and Raman biospectroscopy and density functional theory (DFT) investigation of vibronic–mode coupling structure in vibrational spectra analysis: A spectroscopic study on an anti–HIV drug, *Cientific Drug Delivery Research*, **1(2)**, 11–16.

313. Heidari, A., Esposito, J., Caissutti, A. (2019) Cobrotoxin time–resolved absorption and resonance FT–IR and Raman biospectroscopy and density functional theory (DFT) investigation of vibronic–mode coupling structure in vibrational spectra analysis, *Trends in Res.*, **3(1)**, 1–13.

314. Heidari, A., Esposito, J., Caissutti, A. (2019) Cylindrospermopsin time–resolved absorption and resonance FT–IR and Raman biospectroscopy and density functional theory (DFT) investigation of vibronic–mode coupling structure in vibrational spectra analysis, *Trends in Res.* **3(1)**, 1–14.

315. Heidari, A., Esposito, J., Caissutti, A. (2019) Anthrax toxin time–resolved absorption and resonance FT–IR and Raman biospectroscopy and density functional theory (DFT) investigation of vibronic–mode coupling structure in vibrational spectra analysis, *Trends in Res.* **3(1)**, 1–14.

316. Heidari, A., Schmitt, K., Henderson, M., Besana, E. (2019) Investigation of moscovium nano-particles as anti–cancer nano drugs for human cancer cells, tissues and tumors treatment, *Elixir Appl. Chem*., **137A**, 53943–53963.

317. Heidari, A., Schmitt, K., Henderson, M., Besana, E. (2019) Study of function of the beam energy and holmium nanoparticles using 3D finite element method (FEM) as an optothermal human cancer cells, tissues and tumors treatment, *European Journal of Advances in Engineering and Technology*, **6(12)**, 34–62.

318. Heidari, A., Schmitt, K., Henderson, M., Besana, E. (2019) Human cancer cells, tissues and tumors treatment using dysprosium nanoparticles, *Asian J. Mat. Chem*., **4(3–4)**, 47–51.

319. Heidari, A., Schmitt, K., Henderson, M., Besana, E. (2019) Simulation of interaction of synchrotron radiation emission as a function of the beam energy and plutonium nanoparticles using 3D finite element method (FEM) as an optothermal human cancer cells, tissues and tumors treatment, *J. Cancer Research and Cellular Therapeutics*, **2(4)**, 1–19.

320. Heidari, A., Schmitt, K., Henderson, M., Besana, E. (2019) Study of gadolinium nanoparticles delivery effect on human cancer cells, tissues and tumors treatment under synchrotron radiation, *Applied Chemistry*, **2(2)**, 55–97.

321. Heidari, A., Schmitt, K., Henderson, M., Besana, E., Gobato, R. (2020) Pros and cons of livermorium nanoparticles for human cancer cells, tissues and tumors treatment under synchrotron radiation using Mathematica 12.0, *Parana Journal of Science and Education (PJSE)* **6(1)**, 1–31.

322. Gobato, R., Gobato, M. R. R., Heidari, A., Mitra, A. (2020) Challenging giants. Hartree–Fock methods analysis protonated rhodochrosite crystal and potential in the elimination of cancer cells through synchrotron radiation, *Biomed. J. Sci. & Tech. Res.*, **25(1)**, 18843–18848.

323. Heidari, A., Schmitt, K., Henderson, M., Besana, E. (2019) Simulation of interaction between ytterbium nanoparticles and human gum cancer cells, tissues and tumors treatment under synchrotron radiation, *Dent Oral Maxillofac Res.*, **5(5)**, 1–18.

324. Heidari, A., Schmitt, K., Henderson, M., Besana, E. (2019) Modelling of interaction between curium nanoparticles and human gum cancer cells, tissues and tumors treatment under synchrotron radiation, *Dent Oral Maxillofac Res.*, **5(5)**, 1–18.

325. Heidari, A., Schmitt, K., Henderson, M., Besana, E. (2019) Study of berkelium nanoparticles delivery effectiveness and efficiency on human gum cancer cells, tissues and tumors treatment under synchrotron radiation, *Dent Oral Maxillofac Res.*, **5(5)**, 1–18.

326. Heidari, A., Schmitt, K., Henderson, M., Besana, E. (2019) Fermium nanoparticles delivery mechanism in human gum cancer cells, tissues and tumors treatment under synchrotron radiation, *Dent Oral Maxillofac Res.*, **5(5)**, 1–17.

327. Heidari, A., Schmitt, K., Henderson, M., Besana, E. (2019) Advantages of lawrencium nanoparticles for human gum cancer cells, tissues and tumors treatment under synchrotron radiation, *Dent Oral Maxillofac Res.*, **5(5)**, 1–18.

328. Heidari, A., Schmitt, K., Henderson, M., Besana, E. (2019) Pros and cons of the roentgenium nanoparticles for human gum cancer cells, tissues and tumors treatment under synchrotron radiation, *Dent Oral Maxillofac Res.*, **5(5)**, 1–17.

329. Heidari, A., Schmitt, K., Henderson, M., Besana, E. (2019) Imagery of flerovium nanoparticles delivery process in human gum cancer cells, tissues and tumors treatment under synchrotron radiation, *Dent Oral Maxillofac Res.*, **5(5)**, 1–18.

330. Heidari, A., Esposito, J., Caissutti, A. (2019) Maitotoxin time–resolved absorption and resonance FT–IR and Raman biospectroscopy and density functional theory (DFT) investigation of vibronic–mode coupling structure in vibrational spectra analysis: A spectroscopic study on an anti–gum cancer drug, *Dent Oral Maxillofac Res.*, **5(5)**, 1–16.

331. Heidari, A., Esposito, J., Caissutti, A. (2019) Batrachotoxin time–resolved absorption and resonance FT–IR and Raman biospectroscopy and density functional theory (DFT) investigation of vibronic–mode coupling structure in vibrational spectra analysis: A spectroscopic study on an anti–gum cancer drug, *Dent Oral Maxillofac Res.*, **5(6)**, 1–16.

332. Heidari, A., Schmitt, K., Henderson, M., Besana, E. (2019) Hafnium nanoparticles and their roles and applications in human gum cancer cells, tissues and tumors treatment under synchrotron radiation, *Dent Oral Maxillofac Res*, **5(6)**, 1–17.

333. Heidari, A., Schmitt, K., Henderson, M., Besana, E. (2019) Dramaturgy of technetium nanoparticles delivery process in human gum cancer cells, tissues and tumors treatment under synchrotron radiation, *Dent Oral Maxillofac Res.*, **5(6)**, 1–19.

334.Heidari, A., Schmitt, K., Henderson, M., Besana, E. (2019) Computational approach to interaction between synchrotron radiation emission as a function of the beam energy and ruthenium nanoparticles in human gum cancer cells, tissues and tumors treatment, *Dent Oral Maxillofac Res.*, **5(6)**, 1–18.

335. Heidari, A., Schmitt, K., Henderson, M., Besana, E. (2019) Appearance check of rhodium nanoparticles delivery trend in human gum cancer cells, tissues and tumors treatment under synchrotron radiation, *Dent Oral Maxillofac Res.*, **5(6)**, 1–19.

336. Heidari, A., Schmitt, K., Henderson, M., Besana, E. (2019) Orientation rhenium nanoparticles delivery target on human gum cancer cells, tissues and tumors under synchrotron radiation, *Dent Oral Maxillofac Res.*, **5(6)**, 1–18.

337. Heidari, A., Schmitt, K., Henderson, M., Besana,

E. (2019) Drug delivery systems (DDSs) of osmium nanoparticles on human gum cancer cells, tissues and tumors treatment under synchrotron radiation, *Dent Oral Maxillofac Res.*, **5(6)**, 1–18.

338. Heidari, A., Schmitt, K., Henderson, M., Besana, E. (2019) Development of successful formulations for oral drug delivery concepts of iridium nanoparticles in human gum cancer cells, tissues and tumors treatment under synchrotron radiation, *Dent Oral Maxillofac Res.*, **5(6)**, 1–19.

339. Heidari, A., Schmitt, K., Henderson, M., Besana, E. (2020) Classification of drug delivery system of niobium nanoparticles in human gum cancer gum cells, tissues and tumors treatment under synchrotron radiation, *Dent Oral Maxillofac Res.*, **6(1)**, 1–17.

340. Heidari, A., Schmitt, K., Henderson, M., Besana, E. (2020) Types of drug delivery system slideshare of protactinium nanoparticles in human gum cancer cells, tissues and tumors treatment under synchrotron radiation, *Dent Oral Maxillofac Res.*, **6(1)**, 1–17.

341. Heidari, A., Schmitt, K., Henderson, M., Besana, E. (2020) New drug delivery system in pharmaceutics of neptunium nanoparticles in human gum cancer cells, tissues and tumors treatment under synchrotron radiation, *Dent Oral Maxillofac Res.*, **6(1)**, 1–18.

342. Heidari, A., Schmitt, K., Henderson, M., Besana, E. (2020) Drug delivery describes the method and approach to delivering drugs or pharmaceuticals and other xenobiotics to their site of action within radon nanoparticles effects on human gum cancer cells, tissues and tumors treatment under synchrotron radiation, *Dent Oral Maxillofac Res.*, **6(1)**, 1–18.

343. Heidari, A., Schmitt, K., Henderson, M., Besana, E. (2020) Applications of oganesson nanoparticles in increasing rapidly with the promise of targeted and efficient drug delivery in human gum cancer cells, tissues and tumors treatment under synchrotron radiation, *Dent Oral Maxillofac Res.*, **6(1)**, 1–19.

344. Heidari, A., Schmitt, K., Henderson, M., Besana, E. (2020) Wheeler–Feynman time– symmetric study of effectiveness and efficiency of terbium nanoparticles delivery mechanism in human cancer cells, tissues and tumors under synchrotron radiation, *Frontiers Drug Chemistry Clinical Res.*, **3(1)**, 1–13.

345. Heidari, A., Schmitt, K., Henderson, M., Besana, E. (2019) Simulation of interaction of synchrotron radiation emission as a function of the beam energy and californium nanoparticles using 3D finite element method (FEM) as an optothermal human cancer cells, tissues and tumors treatment, *Oncol Res: Open Acce*., **1(1)**, 1–17.

346. Heidari, A. (2019) Market analysis of glycobiology and glycochemistry 2020, *J. Genet Disor. Genet Rep*., **8**, 1.

347. Heidari, A., Schmitt, K., Henderson, M., Besana, E. (2020) Synchrotron radiation emission as a function of the beam energy and thorium nanoparticles, *International Medicine*, **2(1)**, 67–73.

348. Heidari, A., Schmitt, K., Henderson, M., Besana, E. (2020) Stochastic study of relativistic lutetium nanoparticles moving in a quantum field of synchrotron radiation emission when charged lutetium nanoparticles are accelerated radially in human cancer cells, tissues and tumors treatment**,** *Frontiers Drug Chemistry Clinical Res.*, **3(1)**, 1–15.

349. Heidari, A., Caissutti, A., Henderson, M., Schmitt, K., Besana, E., Esposito, J., Peterson, V. (2020) Recent new results and achievements of california south university (CSU) bioSpectroscopy core research laboratory for COVID–19 or 2019–nCoV treatment: Diagnosis and treatment methodologies of "Coronavirus", *Journal of Current Viruses and Treatment Methodologies*, **1(1)**, 3–41.

350. Heidari, A., Schmitt, K., Henderson, M., Besana, E. (2020) Study of human cancer cells, tissues and tumors treatment through interaction between synchrotron radiation and cerium nanoparticles, *Sci. Lett*., **8(1)**, 7–17.

351. Heidari, A., Schmitt, K., Henderson, M., Besana, E. (2020) Study of characteristic polarization and the frequencies generated in interaction of synchrotron radiation emission and actinium nanoparticles in human cancer cells, tissues and tumors treatment process, *Parana Journal of Science and Education (PJSE)*, **6(3)**, 13–47.

352. Heidari, A., Schmitt, K., Henderson, M., Besana, E. (2020) Californium nanoparticles and human cancer treatment: Commemorating the 100th (1920–2020) anniversary of the california south university (CSU), *Parana Journal of Science and Education (PJSE)*, **6(3)**, 48–83.

353. Gobato, R., Gobato, M. R. R., Heidari, A., Mitra, A., Dosh, I. K. K. (2020) Secret messages in enigmatic playful texts, *ABEB*, **4(2)**, 1–10.

354. Heidari, A., Schmitt, K., Henderson, M., Besana, E. (2020) A Chemical review on cancer immunology and immunodeficiency, *International Journal of Advanced Chemistry*, **8(1)**, 27–43.

355. Heidari, A., Peterson, V. (2020) A comprehensive review on functional roles of cancerous immunoglobulins and potential applications in cancer immunodiagnostics and immunotherapy, *International Journal of Advanced Chemistry*, **8(1)**, 44–58.

356. Heidari, A., Peterson, V. (2020) An encyclopedic review on stereotactic hypofractionated radiotherapy, re–irradiation and cancer genome research, *International Journal of Advanced Chemistry*, **8(1)**, 59–74.

357. Heidari, A., Peterson, V. (2020) A pervasive review on biomarker in cervical intraepithelial lesions and carcinoma, *International Journal of Advanced Chemistry*, **8(1)**, 75–88.

358. Heidari, A., Schmitt, K., Henderson, M., Besana, E. (2020) Hereditary immunity in cancer, *International Journal of Advanced Chemistry*, **8(1)**, 94–110.

359. Heidari, A., Gobato, R., Gobato, M. R. R., Mitra, A. (2020) Hartree–Fock methods analysis protonated rhodochrosite crystal and potential in the elimination of cancer cells through synchrotron radiation using small–angle x–ray scattering (SAXS), ultra–small angle x–ray scattering (USAXS), fluctuation x–ray scattering (FXS), wide–angle x–ray scattering (WAXS), grazing–incidence small–angle x–ray scattering (GISAXS), grazing–incidence wide–angle x–ray scattering (GIWAXS) and small–angle neutron scattering (SANS), *AJAN*, **1(1)**, 1–8.

360. Heidari, A., Gobato, R., Dosh, I. K. K., Mitra, A., Gobato, M. R. R. (2020) Single layer bioinorganic membrane using the kurumi molecule, *AJAN*, **1(1)**, 16–20.

361. Heidari, A., Schmitt, K., Henderson, M., Besana, E. (2020) Study of pulsed time structure of nobelium nanoparticles in human cancer cells, tissues and tumors treatment process which covers from microwaves to hard x–rays, *Dent Oral Maxillofac Res.*, **6(2)**, 1–17.

362. Heidari, A., Schmitt, K., Henderson, M., Besana, E. (2020) Abraham–Lorentz–Dirac force approach to interaction of synchrotron radiation emission as a function of the beam energy and rutherfordium nanoparticles using 3D finite element method (FEM) as an optothermal human cancer cells, tissues and tumors treatment, *Dent Oral Maxillofac Res.*, **6(2)**, 1–17.

363. Heidari, A., Schmitt, K., Henderson, M., Besana, E. (2020) Liénard–Wiechert field study of interaction of synchrotron radiation emission as a function of the beam energy and seaborgium nanoparticles using 3D finite element method (FEM) as an optothermal human cancer cells, tissues and tumors treatment, *Dent Oral Maxillofac Res.*, **6(2)**, 1–17.

364. Heidari, A., Schmitt, K., Henderson, M., Besana, E. (2020) Lorenz gauge, electric and magnetic fields study of interaction of gravitationally accelerating ions through the super contorted 'tubular' polar areas of magnetic fields and hassium nanoparticles, *Dent Oral Maxillofac Res.*, **6(2)**, 1–18.

365. Heidari, A., Schmitt, K., Henderson, M., Besana, E. (2020) Scalar Abraham–Lorentz–Dirac–Langevin equation, radiation reaction and vacuum fluctuations simulation of interaction of synchrotron radiation emission as a function of the beam energy and tennessine nanoparticles using 3D finite element method (FEM) as an optothermal human cancer cells, tissues and tumors treatment, *Dent Oral Maxillofac Res.*, **6(2)**, 1–17.

366. Heidari, A., Schmitt, K., Henderson, M., Besana, E. (2020) The dynamics and quantum mechanics of an interaction of synchrotron radiation emission as a function of the beam energy and meitnerium nanoparticles using 3D finite element method (FEM) as an optothermal human cancer cells, tissues and tumors treatment, *Dent Oral Maxillofac Res.*, **6(2)**, 1–17.

367. Heidari, A. (2020) Future advanced study of thin layers of DNA/RNA hybrid molecule nanostructure, *J. Mol Nanot Nanom*, **2(1)**, 110–116.

368. Heidari, A. (2020) Study of thin layers of cadmium oxide (CdO) nanostructure, *Nano Prog.*, **2(3)**, 1–10.

369. Heidari, A. (2020) Effect of solvent on non–linear synchrotron absorption of multi–walled carbon nanotubes (MWCNTs) with DNA/RNA function, *Sci. Int. (Lahore)*, **32(3)**, 291–315.

370. Kashi, A. S. Y., Khaledi, S., Houshyari, M. (2016) CT simulation to evaluate of pelvic lymph node coverage in conventional radiotherapy fields based on bone and vessels landmarks in prostate cancer patients, *Iran J. Cancer Prev.*, **9(3),** 6233.

371. Kashi, A. S. Y., Razzaghdoust, A., Rakhsha, A. (2017) A comparative study of treatment toxicities between FOLFOX 4 and modified FOLFOX 6 in Iranian colorectal cancer patients, *Iran J. Cancer Prev*., **10(1)**, 9429.

372. Kashi, A. S. Y., Yazdanfar, S., Esmaeil Akbari, M., Rakhsha, A. (2017) Triple negative breast cancer in Iranian women: Clinical profile and survival study, *Int. J. Cancer Manag*, **10(8)**, 10471.

373. Kashi, A. S. Y., Montazeri, R., Rakhsha, A. (2018) Clinical outcome and prognostic factors in Iranian breast cancer patients after neoadjuvant chemotherapy: A comparative matched study, *Int. J. Cancer Manag*, **11(5)**, 67739.

374. Rakhsha, A., Anvari, A., Razzaghdoust, A., Kashi, A. S. Y. (2017) Clinical outcome and prognostic factors for very young patients with breast cancer: A comparative matched single institution study in Iran, *Int. J. Cancer Manag*, **10(9)**, 11772.

375. Rakhsha, A., Kashi, A. S. Y., Hoseini, A. M. (2015) Evaluation of survival and treatment toxicity with high–dose–rate brachytherapy with cobalt 60 in carcinoma of cervix, *Iran J. Cancer Preven*, **8 (4)**, 3573.20.

376. Kashi, A. S. Y., Mofid, B., Mirzaei, H. R., Azadeh, P. (2010) Overall survival and related prognostic factors in metastatic brain tumors treated with whole brain radiation therapy, *Research Journal of Medical Sciences*, **4(3)**, 213–216.

377. Fooladi, E., Razavizadeh, B. M., Noori, M., Kakooei, A. (2020) Application of carboxylic acid–functionalized of graphene oxide for electrochemical simultaneous determination of tryptophan and tyrosine in milk, *SN Appl. Sci.*, **2**, 527.

378. Sadeghi, S., Fooladi, E., Malekaneh, M. (2015) A new amperometric benzaldhyde biosensor based on aldehyde oxidase immobilized on Fe_3O_4–grapheneoxide/polyvinylpyrrolidone/polyaniline nanocomposite, *Electroanalysis*, **27(1)**, 242–252.

379. Sadeghi, S., Fooladi, E., Malekaneh, M. (2014) A new amperometric biosensor based on Fe_3O_4/polyaniline/laccase/chitosan biocomposite–modified carbon paste electrode for determination of catechol in tea leaves, *Applied Biochemistry and Biotechnology*, **175(3)**, 1603–1616.

380. Sadeghi, S., Fooladi, E., Malekaneh, M. (2014) A nanocomposit/crude extract enzyme–based xanthine biosensor, *Analytical Biochemistry*, **464**, 51–59.

381. Gergeroglu, H., Yildirim, S., Ebeoglugil, M. F. (2020) Nano–carbons in biosensor applications: An overview of carbon nanotubes (CNTs) and fullerenes (C_{60}), *SN Appl. Sci.*, **2**, 603.